

POLYMER COLLOIDS FOR CATALYSIS IN  
FLUOROUS MEDIA AND FOR COLLOIDAL  
CRYSTALLINE ARRAYS

By

RANGARANI KARNATI

Bachelor of Science in Chemistry  
Nagarjuna University  
Guntur, India  
1986

Master of Science in Synthetic Organic Chemistry  
Andhra University  
Vizag, India  
1990

Master of Technology in Bio-technology  
Jawaharlal Nehru Technological University  
Hyderabad, India  
1993

Submitted to the Faculty of the  
Graduate College of the  
Oklahoma State University  
in partial fulfillment of  
the requirements for  
the Degree of  
DOCTOR OF PHILOSOPHY  
May, 2009

POLYMER COLLOIDS FOR CATALYSIS IN  
FLUOROUS MEDIA AND FOR COLLOIDAL  
CRYSTALLINE ARRAYS

Thesis Approved:

Warren T. Ford

---

Thesis Adviser

---

K. Darrell Berlin

---

Richard A. Bunce

---

LeGrande M. Slaughter

---

Robert L. Matts

---

A. Gordon Emslie

---

Dean of the Graduate College

## PREFACE

Polymer colloids are the dispersions of solid particles in liquid media with size in the range of 20-1000 nm, also known as polymer latexes. One of the greatest application of polymer latexes in industry is for coating materials. Paints are used as a coating to protect or decorate a surface. This research introduces new applications of polymer latexes in fluorinated solvents and in water as catalysts for the decomposition of toxic organic compounds and for packing colloidal crystalline filters for the filtration purposes.

Uniformly charged polymer latexes in water and oil dispersions can act as phase transfer catalysts (PTC) for the decomposition of toxic organic compounds. A PTC is a catalyst which facilitates the migration of a reactant in a heterogeneous system from one into another phase where reaction can take place. This would lead to the reaction of charged reactants often insoluble in oil with uncharged reagents. In this work we have synthesized polymer latexes in fluorinated solvents. We discovered that only microwave heating gave stable colloids. Regular heating gave foamy solids. We measured the rates of reactions in the fluorinated solvents using polymer particles and without particles to know their optimum catalytic activity for the decomposition of toxic compounds. We observed that the polymer particles slightly increased the rate of reaction compared to the control experiment with no particles in fluorinated solvent.

Polymeric particles in water and oil dispersions can also self assemble to form colloidal crystals (CC). The CC formation depends upon the concentration of the

particles in the liquid dispersion, particle size, charge and the ionic impurities. Previous studies on making CC's using various latexes in water have focused on defects of the film but did not address the morphology of the packing. In this work we synthesized latexes in water to make size selective CC's for filtration of nanometric particles and solutes from the water. We used particle settling and sonication methods to pack CC's using uniform latex particles. Scanning electron microscopic images showed that the top surface of our CC film does not have well ordered regions of particles for the size selective filtration.

## ACKNOWLEDGMENTS

I would like to express my deep appreciation to my research advisor, Dr. Warren T. Ford for his understanding, guidance, patience, and work ethics throughout my research. I wish to extend my appreciation to my colleagues in our research group for their friendship, and support. I am very grateful to Dr. Darrell Berlin, Dr. Richard Bunce, Dr. LeGrande Slaughter, and Dr. Robert L. Matts for serving on my research committee.

I must thank Dr. Young Hie Kim, Dr. Susheng Tan, and Dr. Benjamin J. Lawrence for their friendship and research assistance during my stay.

I would also give my special appreciation to my parents Mr. Subbarao and Mrs. Lakshmi for their love, encouragement, and support throughout my study. I also wish to thank my sisters and brothers for their inspiration and love through all my education. I would also thank my husband, Vishweshwarrao Karnati, and my son, Maneesh Karnati, for their never ceasing encouragement, love, and support.

Finally, I would like to acknowledge the Department of Chemistry for providing me teaching assistant ship during my graduate study. I would like to thank Dr. Ford and Defense Threat Reduction Agency via the US Army Research Office for the financial support as research assistant during the course of my study at Oklahoma State University.

## TABLE OF CONTENTS

Chapter	Page
I. INTRODUCTION.....	1
Polymer Latexes.....	2
Phase Transfer Catalysis.....	3
Polymer Colloids as Phase Transfer Catalysts.....	4
Applications of Polymer Latexes.....	8
Objectives of Research.....	9
Colloidal Crystals.....	10
Formation of Colloidal Crystals.....	11
Ordering of Colloidal Crystals.....	11
Applications of Colloidal Crystals.....	13
Objectives of Research.....	14
References.....	15
II. SYHNTHESES OF 2-ETHYLHEXYL METHACRYLATE LATEXES BY DISPERSION POLYMERIZATION AND USE AS CATALYTIC MEDIA.....	18
Introduction.....	18
Results.....	22
Dispersion Polymerization.....	22
Conversion of VBC Units to Quaternary Ammonium Ions.....	28
Hydrolysis of PNPB by Solid and Stable Copolymers.....	32
Hydrolysis of PNPB by Solid Copolymers in Cl <sup>-</sup> Form in NaOH Solution.....	32
Hydrolysis of PNPB by Solid Copolymers in Cl <sup>-</sup> Form in HFE-7200.....	33
Hydrolysis of PNPB by Solid Copolymers in OH <sup>-</sup> Form in HFE-7200.....	34
Hydrolysis of PNPB by Stable Copolymer in Cl <sup>-</sup> Form in HFE-7200 and Borate Buffer Mixture.....	36
Discussion.....	41
Summary.....	47
Experimental.....	48
References.....	58
III. SYNTHESIS OF POLY (METHYL METHACRYLATE ) CORE-SHELL LATEXES FOR COLLOIDAL CRYSTALLINE FILTER.....	61

Chapter	Page
Introduction.....	61
Results.....	63
Batch Polymerization.....	64
Seeded Emulsion Polymerization .....	65
Shell Growth by Starved Semi-Continuous Polymerization .....	67
Colloidal Crystalline Filters .....	71
Gravitational Sedimentation and Solvent Evaporation.....	71
Fluidic Cell Approach by Sonication Assisted Packing .....	74
Discussion .....	76
Summary .....	77
Experimental .....	78
References.....	84

## LIST OF TABLES

### Chapter I

Table	Page
1. Relative Rate Constants of Hydrolysis of PNP-Hexanoate .....	5

### Chapter II

Table	Page
1. EHMA Dispersion Polymers .....	25
2. Compositions of Quaternary Ammonium Ion Functionalized Polymers .....	28
3. Concentrations of $\text{Cl}^-$ , $\text{OH}^-$ , and Wet Ratios for all Solid Copolymers .....	33
4. Hydrolysis of PNPH by Wet Solid Copolymers.....	35
5. Hydrolysis of PNPH by Stable Polymer Particles .....	40
6. Decrease in $t_{1/2}$ with Increase in Contact Time/ Stirring.....	39

### Chapter III

Table	Page
1. Particle Diameters for PMMA Core, Seeded Core and Core-shell Latexes.....	70



## LIST OF FIGURES

### Chapter I

Figure	Page
1. Conversion of alkyl halide to cyanide by tetrabutylammonium ion.....	3

### Chapter II

Figure	Page
1. Monomer conversion vs. time for solution copolymerization of a 61/39 mol percent mixture of EHMA and OFPM .....	26
2. SEM image of cross-linked dispersion polymer particles .....	27
3. Optical microscopic images of quaternized solid polymers: (a) EHMA-OFPM-TMA ( <b>7</b> ), (b) EHMA-PFDM-TMA ( <b>8</b> ).....	29
4. FT-IR spectra of 2-EHMA cross-linked copolymers by microwave (top) and conventional (bottom) polymerizations: (a) before quaternization, (b) after quaternization .....	30
5. Potentiometric curve for quaternized copolymer <b>7</b> vs AgNO <sub>3</sub> .....	31
6. Absorbance of PNPO <sup>-</sup> from hydrolysis of PNPB in borate buffer/HFE-7200 without stirring at 25 °C: (a) with no polymer particles, (b) 0.16 mg of particles, (c) 1.6 mg of particles .....	37
7. Hydrolysis of PNPB in a 3-phase mixture consisting of polymer particles, HFE-7200, and pH 9.4 borate buffer .....	39
8. Appearance of PNPO <sup>-</sup> absorption at 400 nm in the aqueous phase: (a) with no particles, (b) with 2 mg (50 μL) of particles .....	40
9. Mechanism for the hydrolysis of PNPB in polymer supported phase transfer catalysis.....	46

### Chapter III

Figure	Page
1. AFM image of PMMA core latex of 400 nm on mica surface .....	65
2. AFM image of sub-micron PMMA seed growth latex of 500 nm on mica surface.....	67
3. SEM image of sub-micron PMMA seeded core latex .....	67
4. AFM image of PMMA core-shell latex of 555 nm on mica surface .....	69
5. SEM image of PMMA core-shell latex of 555 nm on silica surface .....	69
6. LCM's packing by gravitation sedimentation by solvent evaporation .....	72
7. SEM image of LCM made by gravitational sedimentation by solvent evaporation with no Texanol: (a) before annealing, (b) after annealing.....	73
8. SEM image of LCM: (a) center, (b) the edge .....	74
9. SEM image of LCM packed by gravitational sedimentation by solvent evaporation with 10 wt % Texanol.....	74
10. (a) Schematic diagram of fluidic cell, (b) Experimental setup showing the packing cells on the sonicator. (c) Packed cell constructed from Mylar film of 130 $\mu\text{m}$ .....	75
11. SEM image of the top surface of the LCM developed by sonication assisted method after annealing .....	76

## LIST OF SCHEMES

### Chapter I

Scheme	Page
1. Hydrolysis of <i>p</i> -nitrophenyl alkanoates in basic buffer .....	5
2. Decarboxylation of 6-nitrobenzisoxazole-3-carboxylate.....	6

### Chapter II

Scheme	Page
1. Fluorinated solvent HFE-7200.....	19
2. Structure of 2-EHMA cross-linked copolymer and the fluoromonomers .....	23
3. Synthesis of the poly (perfluorooctyl acrylate).....	28
4. Hydrolysis of <i>p</i> -nitrophenyl hexanoate in borate buffer, polymer particles, and HFE-7200.....	36

### Chapter III

Scheme	Page
1. Batch polymerization of methyl methacrylate .....	65
2. Seeded emulsion polymerization of methyl methacrylate .....	66
3. Shell growth by starved semi-continuous polymerization.....	68

## LIST OF SYMBOLS AND ABBREVIATIONS

<b>AA</b>	Acrylic acid
<b>AFM</b>	Atomic force microscopy
<b>AMA</b>	Allyl methacrylate
<b>BA</b>	Butyl acrylate
<b>CMC</b>	Critical micelle concentration
<b>DLS</b>	Dynamic light scattering
<b>DS2</b>	Decontamination Solution
<b>DVB</b>	Divinylbenzene
<b>EHMA</b>	2-Ethylhexyl methacrylate
<b>GMA</b>	Glycidyl methacrylate
<b>HFE-7100</b>	Nonafluorobutyl methyl ether
<b>HFE-7200</b>	Nonafluorobutyl ethyl ether
<b>LCM</b>	Latex composite membrane
<b>MMA</b>	Methyl methacrylate
<b>NBIC</b>	6-nitrobenzoxazole-3-carboxylate
<b>OFPM</b>	Octafluoropentyl methacrylate
<b>OM</b>	Optical microscopy
<b>PFDM</b>	Perfluorodecyl methacrylate
<b>PMMA</b>	Poly(methyl methacrylate)

<b>PNPH</b>	<i>p</i> -Nitrophenyl hexanoate
<b>PNPO<sup>-</sup></b>	<i>p</i> -Nitrophenoxide ion
<b>PPFOA</b>	Poly(perfluorooctyl acrylate)
<b>SEM</b>	Scanning electron microscopy
<b>Texanol</b>	2,2,4-Trimethyl-1,2-pentanediol monoisobutyrate
<b>VBC</b>	Vinylbenzyl chloride

## CHAPTER I

### INTRODUCTION

Polymer colloids are the stable suspensions or dispersions of particles of polymeric materials, in a liquid medium, most often water. Associated colloidal dispersions, such as polyelectrolytes,<sup>1-4</sup> anion-exchange resins,<sup>5-6</sup> surfactant micelles,<sup>7-9</sup> and polymer latexes<sup>10-12</sup> have been used as heterogeneous media to enhance the rates of reactions in aqueous media. The basic principle involved in all these systems is that, they facilitate the migration of a reactant in a heterogeneous system from one phase into another phase where reaction can take place. Ionic reactants are often soluble in an aqueous phase but insoluble in an organic phase unless the phase transfer catalyst is present. These heterogeneous catalytic media offers a unique advantage that one can carry out the organic reactions in aqueous media which would otherwise is impossible.

All the above mentioned methods offer distinct advantages and disadvantages over some of the other media. In this chapter, I would like to explain how polymer latexes are made; to explain how polymer latexes are used as phase transfer catalyts in heterogeneous media; to describe at the some of the systems that have been studied using polymer latexes for phase transfer catalysis; and to give limitations and potential applications of polymer latexes as catalytic media.

## **Polymer Latexes**

In general, polymer latexes are stable dispersions of sub-micrometer sized polymer particles in a liquid matrix (usually water). Monodisperse latex dispersions are iridescent and the color of the polymer latex is characteristic and depends on the particle size and the concentration. The latex particles are colloidally stable and do not fall out of the solution due to gravitational forces because of the electrostatic repulsions of the charged sites on the particle surface. The surface charges can arise from the initiator used, adsorbed or grafted surfactants, use of ionic monomers and adsorbed or grafted polymeric species, and hairy charged surfaces with hairs being surfactants or polyelectrolytes.

Latexes are synthesized by either emulsion or dispersion polymerization. A most important feature of the emulsion polymerization is its heterogeneity from beginning to end. An emulsion polymerization mixture consists of monomer phase, surfactant molecules to cluster into micelles with their hydrophobic core being swollen with monomer, and the water soluble initiator. The bulk of the monomer exists in the form of large-size droplets with surfactant molecules adsorbed on their surfaces. Thermal decomposition of the initiator starts polymerization of the small amount of monomer in the aqueous phase. Growing polymer radicals are trapped by monomer-swollen surfactant micelles, which then are the locus of the polymerization and become polymer particles. The particles continue to grow by the diffusion of monomer from droplets through water and into the particles. This process continues until all of the monomer is consumed to give the stable polymer particles. The surfactant stabilizes the particles against

coagulation.<sup>13</sup> Dispersion polymerization differs from emulsion polymerization in that the process starts with a homogeneous solution of monomer, initiator and a polymeric stabilizer. As polymerization proceeds, the stabilizer adsorbs to the particle surface to keep the insoluble polymeric particles dispersed.<sup>14</sup>

## Phase Transfer Catalysis

Phase transfer catalysis describes the use of lipophilic cations such as quaternary ammonium compounds and crown ethers to promote the reactions between uncharged organic substrates and the anions of water soluble salts. The schematic diagram is shown in Figure 1.

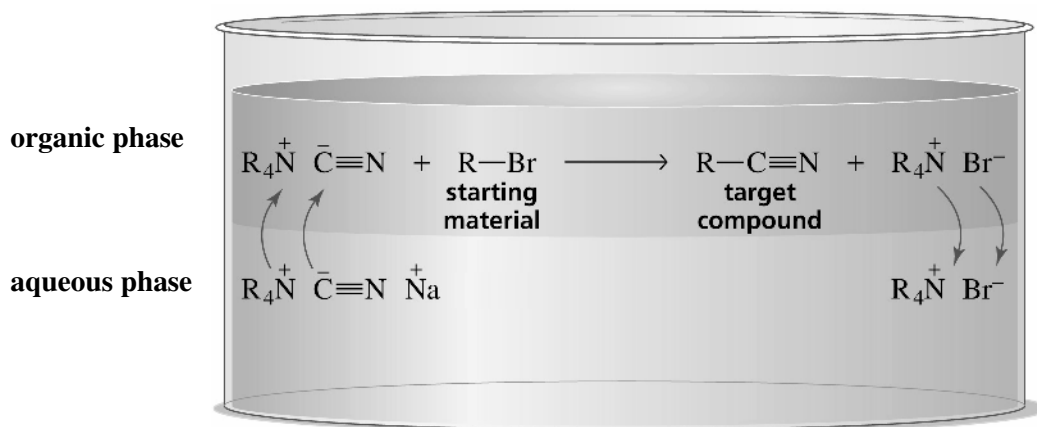


**Figure 1.** Conversion of alkyl halide to alkyl cyanide by tetrabutylammonium ion.

Tetrabutylammonium ion transfers hydroxide ion and cyanide ion from the aqueous phase to organic solution, where the anion reacts with alkyl halide. Similarly cationic polystyrene and poly(2-ethylhexyl methacrylate) colloids have been investigated as phase



transfer catalysts over the past 15 years.<sup>15,16</sup> The cation is generally a quaternary ammonium or phosphonium ion. Kinetics of these reactions within these latexes have been analyzed by an ion exchange model.

### **Polymer Colloids as Phase Transfer Catalysts**

Several reactions have been investigated and have shown that the latexes accelerated the reaction compared with that observed in the absence of latex particles.

**Basic Hydrolysis of *p*-Nitrophenyl Alkanoates.**<sup>15,16</sup> A series of poly(alkyl methacrylate)s such as 2-ethylhexyl methacrylate (EHMA), butyl methacrylate (BMA) and polystyrene latexes (S) containing either trimethylammonium (TMA) or tributylammonium units (TBA) (Table 1) were tested for the hydrolysis of *p*-nitrophenyl alkanoates of various alkyl chain length (Scheme 1) in basic buffer solutions. Kinetics of hydrolysis of *p*-nitrophenyl acetate, hexanoate, and octanoate in borate buffer were measured as functions of particle concentration, pH, and buffer concentration. Partition coefficients and intraparticle second-order rate constants and ion-exchange selectivity coefficients were calculated based on the ion-exchange model.

**Table 1. Relative Rate Constants of Hydrolysis of PNP-Hexanoate<sup>a,b</sup>**

Latex	$k_{\text{obs}}/k_w$	Latex	$k_{\text{obs}}/k_w$
2EHMA-TBA	16.5	S-TBA	12.0
BMA-TBA	15.7	BMA-TMA	6.1
2EHMA-TMA	12.5	S-TMA	2.3

<sup>a</sup> At 30.0 °C in 0.02 M pH 9.38 borate buffer at a latex concentration of 1.2 mg/mL with  $[N^+] = 62 \mu\text{M}$  and substrate concentration of  $4.2 \mu\text{M}$ .  $k_w$  for the reaction in the absence of latex was  $3.26 \times 10^{-4} \text{ s}^{-1}$ . <sup>b</sup> Ref 15, 16.

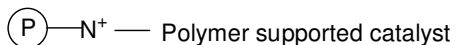
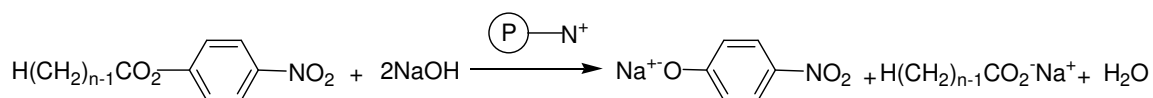
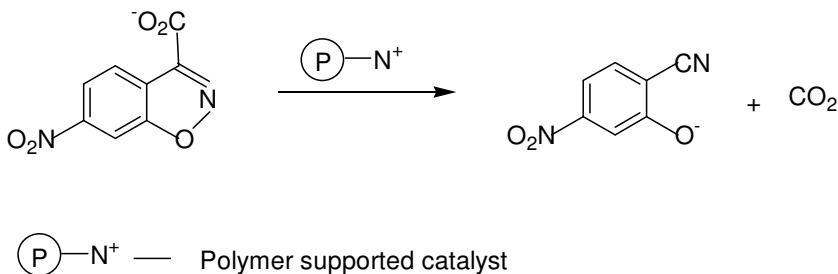
**Scheme 1**

Table 1 shows relative rate constants of polymer supported phase transfer catalytic reactions of *p*-nitrophenyl alkanates. Among all those polystyrene colloidal particles were the least reactive and 2-ethylhexyl methacrylate (EHMA) the most reactive. In methacrylates, catalytic activity increased with increase in size of the alkyl side chain because of increase in partition coefficient of alkanates. The highest catalytic activity of EHMA latexes were due to the larger free volume created by 2-ethylhexyl chains. Another factor is that the tributylamine quaternized latexes were more active than

trimethylamine latexes because the tributylamine increases the aliphatic nature of the latex.

**Decarboxylation of 6-Nitrobenzoxazole-3-carboxylate.**<sup>15,16</sup> The unimolecular decarboxylation of 6-nitrobenzoxazole-3-carboxylate (6-NBIC) by polystyrene and poly(alkyl methacrylates) latexes is shown in Scheme 2. The reaction proceeds 10,400 times faster with ethylhexyl methacrylate-tributylamine latex than with no latex.<sup>15</sup> The rate accelerations are due to both favorable partitioning of 6-NBIC into the latex and faster intraparticle rate constants.

**Scheme 2**



Therefore, systems that have been studied in an ion-exchange model indicate that methacrylate polymer latexes are more active than their polystyrene counterparts. Polymer latexes offer several advantages as colloidal catalysts over the other types of heterogeneous media. I would like to explain how polymer latexes compare to microemulsions, polyelectrolytes, and micelles in heterogeneous catalysis.

**Microemulsions.**<sup>17</sup> Microemulsions are thermodynamically stable dispersions of oil in water, or water in oil that appear transparent because the size of the colloidal

particles or aggregates is so small that the mixture scatters very little visible light. These are stabilized by cosurfactants such as aliphatic alcohols. Microemulsions are sensitive to composition and temperature and any slight changes in one of the parameters cause macroscopic phase separation. If this occurs, the catalytic activity of microemulsion is lost and can not act as phase transfer catalyst to accelerate the rate of reaction. Latexes are discrete particles and are colloidally stable over a wide range of concentrations and temperatures and can be used as catalysts.

**Polyelectrolytes.**<sup>17</sup> Polyelectrolytes (PE) are charged polymer chains. These are soluble in aqueous solutions due to their large amount of charge. A PE has random coil conformations in solution. Amphiphilic PE's arrange themselves like micelles with a lipophilic core and hydrophilic surface. This will enable them to act as phase transfer catalysts to concentrate uncharged organic substrates and anions during the catalysis. PE's lack the structural specificity, and it is hard to isolate the products from the PE's because of their solubility whereas polymer latexes have the definite volume and ease of isolation.

**Micelles.**<sup>17</sup> Micelles are dynamic aggregates of surfactants that constantly undergo association and dissociation. Critical micelle concentration (CMC) is defined as the concentration of surfactants above which micelles are spontaneously formed. Cationic micelles have been studied as catalytic media because they bind anionic reagents and catalysts and also many cationic surfactants are commercially available. Phase transfer catalytic reactions in cationic micelles have been analyzed by a pseudophase ion exchange model.<sup>7,18</sup> The hydrolysis of *p*-nitrophenyl diphenyl phosphate catalyzed by 5-octyloxy *o*-iodosobenzoate is 18,000 times faster than in the absence of the surfactant.<sup>19</sup>

There is no increase in reaction rate unless the surfactant concentration exceeds the CMC. Micelles are not active participants in catalysis but act as a second phase in the reaction mixture to concentrate reactants from surrounding aqueous solution. Polymer latexes are discrete particles and do have the catalytic activity even at very low concentrations. Volume of the latex particles can be determined at any time because of their static nature whereas the volume of the Stern layer at the surface of the micelles needs to be approximated.

### **Applications of Polymer Latexes**

One potentially important use of polymer latexes is for the hydrolysis and neutralization of toxic organophosphates, phosphonates, and fluorophosphonates, which are widely used as insecticides and are stockpiled as chemical warfare agents.<sup>20</sup> As stated earlier, EHMA-TBA latex increased the rate of decarboxylation of 6-NBIC, and polystyrene latexes containing quaternary ammonium ion exchange sites together with anionic *o*-iodosobenzoate markedly increased the hydrolysis rate of the *p*-nitrophenyl diphenyl phosphate (PNDPP). PNDPP is widely used as a model for nerve agents. Hence, latexes might be good choice for the neutralization of stimulants of the contaminants.

Quaternary ammonium ion latexes are highly efficient media for reactions of anionic and uncharged organic species. Cross-linked polymer structures can be converted to positively charged quaternary ammonium salts which can behave like ion-exchange resins. These hydrophobic polymer matrixes able to extract the anions from the aqueous

environment into the particles where the substrate and the reagent have the intimate contact for the phase transfer catalysis to occur.

Recently acrylate polymer latexes containing fluorocarbon moieties have greatly gained in importance as coatings.<sup>21</sup> In these coatings, fluoropolymer functions as a binder for exterior coatings because of their excellent resistance to UV-A and UV-B radiation, as well as to many corrosive chemical agents whereas hydrocarbon acrylate monomer sticks to the substrate. In fact, 2-ethylhexyl methacrylate/fluoropolymer latexes synthesized in fluorinated solvents using microwave dispersion polymerization in this work are a possible alternative for either fluoro coatings or for incineration of stimulants from the contaminated electronic equipment.

### **Objective of the research**

Cationic polymer latexes are known for catalytic media for the alkaline hydrolysis of *p*-nitrophenyl esters by providing a more lipophilic environment into which these compounds and hydroxide ion can partition from the aqueous phase. Most of the research was performed on polystyrene latexes and 2-ethylhexyl methacrylate latexes as heterogeneous catalytic media in aqueous dispersions. There is no work done on 2-ethylhexyl methacrylate latexes as heterogeneous media in fluorinated cleaning solvents for the incineration of stimulants from the contaminated electronic equipment.

The biggest technical challenge of this project is to synthesize stable, quaternized, and cross-linked 2-ethylhexyl methacrylate latexes in fluorinated solvents by emulsion or

dispersion polymerization using fluoro stabilizers. Further, these stable fluorinated dispersions will be tested for catalytic activity using *p*-nitrophenyl alkanoates.

We have explored several synthetic strategies for making stable methacrylate/fluoropolymer dispersions using different or no fluoro stabilizers by dispersion polymerization. We synthesized a stable dispersion in fluorinated solvent by dispersion polymerization using microwave heating. This stable dispersion was tested for its catalytic activity for the hydrolysis of *p*-nitrophenyl hexanoate. We chose *p*-nitrophenyl (PNP) ester because of its availability in wide range of carbon chain lengths, easy to follow the absorbance of *p*-nitrophenoxide by UV-Vis, and the extensive literature on the behavior of PNP esters.

The long term objective of this research is to find a unique and better method to use these stable fluoro dispersions as heterogeneous catalytic media for the hydrolysis of stimulants of the chemical warfare agents. This could provide a better life for military and civilian populations.

## **Colloidal Crystals**

Monodisperse charged spherical colloidal particles in aqueous and non-aqueous dispersions can self assemble into three-dimensional crystal structures known as colloidal crystals.<sup>22-23</sup> These crystal structures depend on the ratio of the sphere diameter to the nearest-neighbor sphere spacing, size, ionic strength, and the concentration of the particles. Since the lattice spacing usually exceeds 100 nm, Bragg diffraction of visible light occurs in colloidal crystals to exhibit iridescence.<sup>22-23</sup>

## **Formation of Colloidal Crystals**

The colloidal crystal formation<sup>24</sup> by particle dispersions is a three step process consisting of:

- (1) the formation of monodisperse colloidal polymer particles,
- (2) ordering of the particles into polyhedrons under the action of surface and capillary forces,
- (3) coalescence of the particles as a result of interdiffusion of polymer chain segments to interconnect the particles in the crystal lattice.

There is abundant literature on monodisperse systems that form colloidal crystals. Monodisperse poly(methyl methacrylate) latexes can be synthesized by emulsion, and dispersion polymerizations.<sup>25-27</sup> The particle size has been controlled by the concentration of the monomers, surfactants and the method of polymerization. In colloidal dispersions, the ordering and orientation of the particles into a crystalline lattice occurs in several stages. Most of the research to date has been aimed at understanding the colloidal crystalline behavior in liquid dispersions.

## **Ordering of Colloidal Crystals**

The transformation of disordered particles in dispersion to ordered colloidal crystal lattice may be due to either steric repulsion or electrostatic repulsion. Steric interactions are due to long polymer chains grafted on to the particle surface, and electrostatic interactions are due to net charges on each sphere arising from ionization of



sulfate groups which are attached during the particle synthesis by emulsion polymerization.<sup>28</sup> At relatively low particle concentrations, the particles will be in a gas-like state and transform to liquid phase and at high concentrations go to a solid-like state to form crystalline or amorphous lattice. Assembling of particles into crystalline lattice can arise either from a boundary or in bulk far from the walls of the vials, and cells. A monolayer of spheres forms two-dimensional arrays (2D). Subsequent application of several layers of particles on to the 2D nucleated sites will form three-dimensional crystal (3D) lattice.

The crystal lattice depends upon the particle concentration and also the order in which the second layer forms on top of the first layer and so on. The resulting crystal lattice by increasing degree of order may be two-dimensional structure < random layer structure < layer structure with one sliding degree of freedom < stacking disorder structure < stacking structure with multivariant periodicity < face-centered-cubic (fcc) structure with (111) twin < normal fcc structure.<sup>29</sup> Therefore, the order of layers in a 3D lattice occurs in ABC or ABA and the crystals are fcc, body-centered-cubic (bcc) or hexagonally closed packing (hcp). The crystals are generally face-centered-cubic (fcc) at high particle volume fractions and low surface charge, and body-centered-cubic (bcc) at low particle volume fractions and high surface charge. Since the lattice spacing is generally > 100 nm in fcc and bcc these lattices cause Bragg diffraction and exhibit iridescence.

## Applications of Colloidal Crystals

Monodisperse polymer colloids have received great attention as a material of choice for a wide range of applications that range from drug delivery to fabrication of photonic devices. In addition colloidal particles have long been used as the major components of industrial products such as foods, inks, paints, paintings and photographic films.<sup>30</sup> Further, these monodisperse polymer colloids can self assemble to colloidal crystals. Colloidal crystals assembled from highly charged polystyrene beads and silica spheres have been known for long time to produce Bragg diffraction of light in the optical region.<sup>31-32</sup> It has been possible to make optical rejection filters. Narrow band width filters made out of monodisperse polystyrene spheres have been used to reject the Rayleigh scattering in Raman spectrometer.<sup>31</sup> Asher and coworkers also developed temperature responsive sensors from poly(N-isopropyl acrylamide), which reversibly dehydrates and thus changes its conformation with a moderate change in temperature.<sup>33</sup> Xia et al. have also studied the photonic properties of 3D photonic crystals obtained from the highly ordered opaline structures of polystyrene beads to produce light emitting diodes (LEDs).<sup>34</sup>

Most of the recent applications derived from the monodisperse colloidal spheres such as photonic papers,<sup>35</sup> and nanoparticle networks for controlled drug delivery,<sup>36,37</sup> are still in the early stage of technical development. Most of these polymer latexes were synthesized in water, which minimizes the use of organic solvents.

## **Objective of the Research**

Though the ordered composite materials fabricated using monodisperse charged colloids hold great promise as optical<sup>32</sup> and photoelectronic devices, sensors, and catalyst supports,<sup>38-40</sup> not much is known about making size-selective filters and their packing morphologies. Most of the studies were conducted on colloidal crystals of silica, polystyrene, and poly(methyl methacrylate) (PMMA) for photonic devices but not on functional materials of core-shell latexes to make filters.

In this research we would like to take the advantage of self assembly nature of monodisperse latex particles to pack latex composite membranes (LCM). Membranes will be fabricated using either by gravitational sedimentation by solvent evaporation or sonication assisted packing techniques. Morphology of the packed particles on the surface of the LCM will be analyzed by SEM. Finally, permeabilities of the composite latex membranes will be measured using a mixture of dextrans having broad size distribution and monodisperse latexes of polystyrene. To achieve our goal of making LCM's we synthesized sub-micron PMMA core-shell latexes consisting of PMMA hard core and the soft shell by seeded and starved semi-continuous emulsion polymerization.

## References

1. Fife, W. K. *Trends. Polym. Sci.* **1995**, *3*, 214-221.
2. Fendler, J. H.; Fendler, E. H. *Catalysis in Micellar and Macromolecular Systems*; Academic: New York, 1975.
3. Zheng, Y.; Knoesel, R.; Galin, J. *Polymer* **1987**, *28*, 2297-2303.
4. Yang, Y.; Engberts, J. *J. Org. Chem.* **1991**, *56*, 4300-4304.
5. Ford, W. T.; Tomoi, M. *Adv. Polym. Sci.* **1984**, *55*, 49-104.
6. Tomoi, M.; Ford, W. T. *Synthesis and Separations Using Functional Polymers*; Sherrington, D. C., Hodge, P., Eds.; Wiley: Chichester, **1988**; pp 181-207.
7. Bunton, C. A.; Savelli, G. *Adv. Phys. Org. Chem.* **1987**, *22*, 213-309.
8. Moss, R.; Alwis, K.; Bizzigotti, G. *J. Am. Chem. Soc.* **1983**, *105*, 681-682.
9. Moss, R.; Kotchevar, A.; Byeong, D. *Langmuir* **1996**, *12*, 2200-2206.
10. Lee, J. J.; Ford, W. T. *J. Am. Chem. Soc.* **1994**, *116*, 3753-3759.
11. Yu, H.; Ford, W. T. *Langmuir* **1993**, *9*, 1999-2007.
12. Lee, J.-J.; Ford, W. T. *J. Org. Chem.* **1993**, *58*, 4070-4077.
13. El-Aasser, M. S.; Sudol, E. D. *In Emulsion Polymerization and Emulsion Polymers*; Lovell, P. A., El-Aasser, M. S., Eds.; Wiley: Chichester, **1997**, pp 37-55.
14. Shiho, H.; Desimone, J. M. *Macromolecules* **2001**, *34*, 1198-1203.
15. Miller, P. D.; Ford, W. T. *Langmuir* **2000**, *16*, 592-596.
16. Miller, P. D.; Spivey, O. H.; Copeland, L. S.; Sanders, R.; Woodruff, A.; Gearhart, D.; Ford, W. T. *Langmuir* **2000**, *16*, 108-114.
17. Ford, W. T.; Miller, P. D. *Microspheres Microcapsules & Liposomes*; Arshady, R.;

- Ed.; Citus: London, **1999**, pp 171-202.
18. Bunton, C. A. Micellar rate effects upon organic reactions; Grätzel, M., Kalyanasundaram, K., Eds.; Marcel Dekker: New York, **1999**; pp 13-48.
  19. Moss, R. A.; Alwis, K. W.; Bizzigotti, G. O. *J. Am. Chem. Soc.* **1983**, *105*, 681-682.
  20. Yang, Y. -C.; Baker, J. A.; Ward, J. R. *Chem. Rev.* **1992**, *92*, 1729-1743.
  21. Sung, Li-P.; Vicini, S.; Ho, L. D.; Hedhli; L.; Olmstead, C.; Wood, A. K. *Polymer* **2004**, *45*, 6639-6646.
  22. Jethmalani J. M.; Ford, W. T. *Chem. Mater.* **1996**, *8*, 2138-2146.
  23. Jethmalani J. M.; Sunkara, H. B.; Ford, W. T. *Langmuir* **1997**, *13*, 2633-2639.
  24. Zosel, A.; Ley, G. *Prog. Colloid. Polym. Sci.* **1996**, *101*, 86-92.
  25. Lee, C. F. *Polymer* **2000**, *41*, 1334-1337.
  26. Lee, C.F. *Colloid. Polym. Sci.* **2002**, *280*, 116-123.
  27. Tamai, H.; Niino, K.; Suzava, T. *J. Coll. Interface. Sci.* **1989**, *131*, 1-3.
  28. Rundquist, A. P.; Photinos, P.; Jagannathan, S.; Asher, A. S. *J. Chem. Phys.* **1989**, *91*(8), 4931-4932.
  29. Sogami, S. I.; Yoshiyama, T. *Phase Transitions* **1990**, *21*, 171-182.
  30. Xia, Y.; Gates, B.; Yin, y.; Lu, Y. *Adv. Mater.* **2000**, *12*, 693-713.
  31. Flaugh, P. L.; O'Donnell, S. E.; Asher, S. A. *Appl. Spectrosc.* **1984**, *38*, 847-853.
  32. Monovoukas, Y.; Gast, A. P. *Langmuir* **1991**, *7*, 460-468.
  33. Pan, G.; Kesavamoorthy, R.; Asher, S. A. *J. Am. Chem. Soc.* **1998**, *120*, 6525-6530.
  34. Park, S. H.; Qin, Y.; Xia, Y. *Adv. Mater.* **1998**, *10*, 1028-1032.
  35. Fudouzi, H.; Xia, Y. *Adv. Mater.* **2003**, *15*, 892-896.
  36. Huang, G.; Gao, J.; Hu, Z.; St. John, J. V.; Ponder, B. C.; Moro, D. *J. Controlled*

*Release* **2004**, *94*, 203-207.

37. Hamilton, B.; Jacobs, J.; Hill, D. A.; Pettifer, R. F.; Teehan, D.; Canhams, L. T.

*Nature (London)* **1997**, *393*, 443-447.

38. Kamenetzky, L. G.; Mangliocco, L. G.; Pinzer, H. P. *Science* **1994**, *263*, 207-210.

39. Yablonoich, E. *Phys. Rev. Lett.* **1987**, *58*, 2059-2062.

40. John, S. *Phys. Rev. Lett.* **1987**, *58*, 2486-2489.

## CHAPTER II

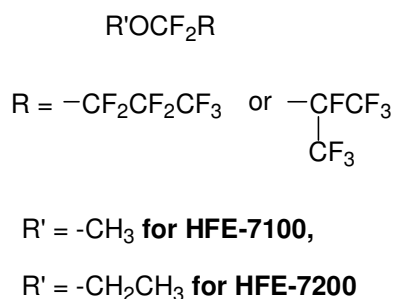
### 2-ETHYLHEXYL METHACRYLATE LATEXES BY DISPERSION POLYMERIZATION FOR USE AS CATALYTIC MEDIA IN FLUORINATED SOLVENTS

#### Introduction

Decontamination of chemical warfare (CW) agents trapped in nooks and crannies of electronic equipment and interiors of vehicles is a challenging task. The most common CW agents are liquids with low to moderate volatility. These CW agents could confine in the electronic equipment and cause threat to human life. Present US Department of Defense decontamination methods are effective for decomposition of CW agents but also damage equipment. Decontamination Solution 2 (DS2) is a toxic, corrosive, and flammable liquid. It has long term storage stability and large operating temperature range (-15 to 125 °F or -26 to 52 °C). This is a basic solution of diethylenetriamine (70 %), ethylene glycol monomethyl ether (28 %), and sodium hydroxide (2 %) and the equipment does not survive with this treatment.<sup>1-2</sup> An alternative for the decomposition of CW agents is noncorrosive Decon Green which is a solution of water, propylene glycol, propylene carbonate, Triton X-100, sodium bicarbonate, sodium molybdate, and 30 % H<sub>2</sub>O<sub>2</sub>.<sup>2</sup> The major disadvantage of this method is that all the components of Decon Green have to be stored in separate containers such as organic solvents and surfactants, hydrogen peroxide, and an aqueous solution of activators and have to be mixed immediately before use in the battle field. In addition, the propylene carbonate in Decon

Green swells/softens the polymeric materials used for the construction of electronics.<sup>3-4</sup> It's a challenging task to find a single method to detoxify all CW agents since their chemistries are different from one another.<sup>1,4-5</sup> We need a unique and less damaging method for decontamination of CW agents from the contaminated equipment. Reactive polymer colloids dispersed in fluorinated cleaning solvents might effectively remove and decompose the CW agent. Fluorinated solvents such as HFE-7100 and HFE-7200 are ideal candidates because of their miscibility with the CW agents, low surface tension, and chemical inertness to all organic materials. These are isomeric mixtures of nonafluorobutyl methyl (HFE-7100) or ethyl (HFE-7200) ethers. The structures of fluorinated solvents are shown in Scheme1. These solvents can penetrate into the nooks and crannies of contaminated equipment and remove the agent absorbed. This mixture will be stirred with reactive polymer colloid (PC) dispersed in fluorinated solvent so that the PC hydrolyzes the stimulant esters to decompose the CW agent without forming a residue on the equipment.

### Scheme 1





The major objective of this research is the synthesis of stable reactive polymer colloids in fluorinated solvents by emulsion or dispersion polymerization and the application of those polymer colloids to hydrolyze phosphate esters in the fluorinated solvents. Interestingly not much literature is present on polymerizations in fluorinated solvents. This might be because of greater interest in use of supercritical carbon dioxide and liquid carbon dioxide for cleaning and for polymer processing as an ultimate solvent for Green Chemistry.<sup>6</sup> The properties of fluorinated solvents and carbon dioxide are similar, and both have very low Hildebrand solubility parameters. Colloidal polymers containing fluorinated particle surfaces are designed to facilitate dispersion into fluorinated solvents. Our research group has shown that cross-linked copolymer particles of 2-ethylhexyl methacrylate with quaternary ammonium ion sites have the highest catalytic activity towards the hydrolysis of *p*-nitrophenyl hexanoate in aqueous buffer solutions.<sup>7</sup> The amphiphilic particle cores contain both hydrocarbon-based polymer to absorb toxic organic compounds and ion exchange sites to bind decontaminating reagents. These hydrated polymer particles swollen twice to its dry volume for the decontamination of CW agents. The core content of these polymer particles is same as polymers that have been effective for decontamination of simulants in aqueous dispersions. The polymer particles contain 20-30 mole percent of quaternary ammonium ion repeat units derived from vinylbenzyl chloride (VBC), 70-80 mole percent of 2-ethylhexyl methacrylate (EHMA, the “solvent monomer”), and 1 percent of divinylbenzene (DVB) as a cross-linker to prevent the dissolution of ionic polymer. EHMA is selected as “solvent monomer” because EHMA polymers have shown the highest catalytic activity for hydrolysis of *p*-nitrophenyl alkanoates in basic buffer

solutions<sup>7</sup> and also absorb larger amounts of organic compounds than other alkyl methacrylate and styrene polymers because of the branched 2-ethylhexyl chains. The fluorinated solvent used for polymerization is HFE-7200 because of its higher boiling point and its greater miscibility towards monomers, initiator, and steric stabilizer than that of HFE-7100 (Scheme 1).

Our initial attempts for the dispersion polymerization of 2-ethylhexyl methacrylate (EHMA), vinylbenzyl chloride (VBC), divinylbenzene (DVB), and fluoroalkyl methacrylate monomers in the solvent nonafluorobutyl ethyl ether (HFE-7200) gave colloiddally unstable polymer particles. We applied microwave heating for the dispersion polymerization of EHMA in HFE-7200 to obtain colloiddally stable polymer particles. The application of microwave radiation as an alternate heat source in synthetic chemistry is a fast growing research area. After the first report on microwave synthesis by Gedye<sup>8</sup> and Giguere<sup>9</sup> in 1986, microwave heating has been accepted as a promising method for rapid volumetric heating, increase in reaction rate,<sup>10-13</sup> high temperature homogeneity, shorter reaction time, and increase in yield<sup>14</sup> compared to conventional heating methods. These unique advantages of microwave –assisted chemistry have opened up the possibility of exploring new conditions for polymerizations. Over the last decade, microwave irradiation has been widely applied to both conventional and controlled free radical polymerizations in bulk,<sup>15-19</sup> solution,<sup>20-21</sup> emulsion,<sup>22-25</sup> and dispersion,<sup>26-27</sup> It is surprising that not much research has been reported on dispersion polymerizations of cross-linked copolymers.

In this chapter, we present the results of microwave vs. conventional heating of two types of processes in polymer synthesis: (1) dispersion polymerization of 2-

ethylhexyl methacrylate (2-EHMA), vinylbenzyl chloride (VBC), and divinylbenzene (DVB) in fluoruous solvent using either fluoromonomer (OFPM (1H,1H,5H-octafluoropentyl methacrylate, or PFDM (1H,1H,2H,2H-perfluorodecyl methacrylate)) or homopolymer (polyperfluorooctyl acrylate (PPFOA) ) as a stabilizer and (2) functional group transformation of the dispersion particles from chloromethyl of VBC groups to quaternary ammonium ions using anhydrous trimethylamine. The structures of the quaternized 2-EHMA cross-linked copolymer and the fluoromonomers (OFPM and PFDM) are shown in Scheme 2. Conventional polymerizations and quaternizations gave solid polymers. Microwave polymerization and quaternization gave both stable colloidal dispersions and more efficient functional group conversion with shorter reaction times.

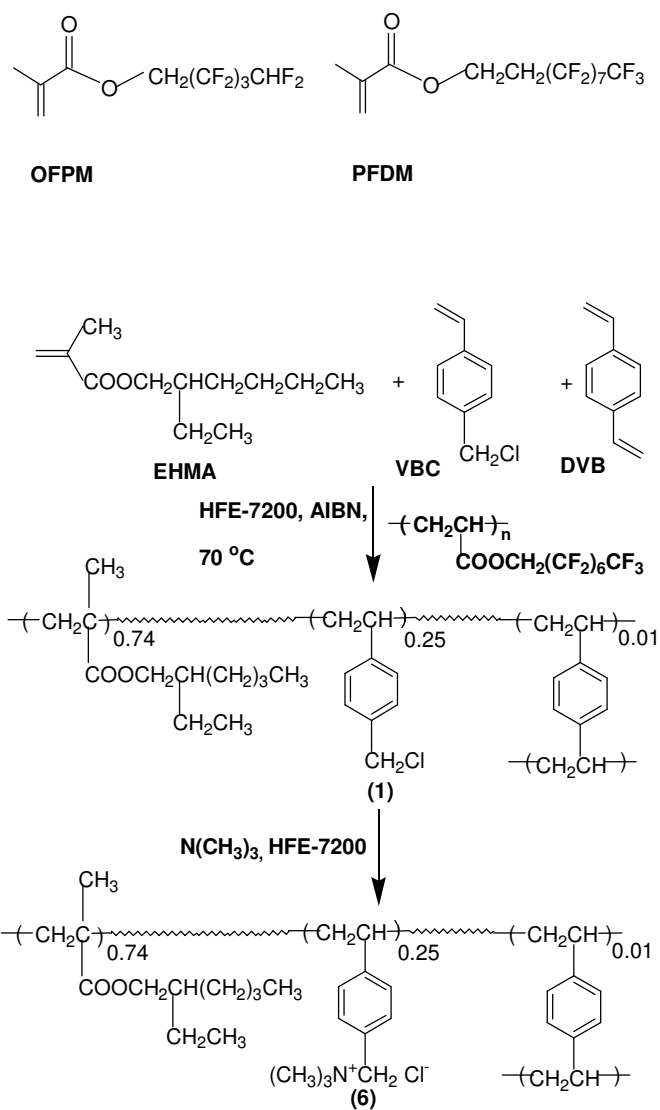
Stable polymer particle cores loaded with chloride ion were tested for the hydrolysis of *p*-nitrophenyl alkanoates in basic buffer solutions. The most effective polymer core loaded with chloride ion can be easily exchanged with hydroxide, bicarbonate, or molybdate ions to do decontamination kinetic experiments.

## Results

**Dispersion Polymerization.** A major objective of this research was to synthesize stable EHMA cross-linked copolymers in fluorinated solvents by dispersion polymerization and then converting  $-\text{CH}_2\text{Cl}$  group to  $-\text{CH}_2\text{N}^+(\text{CH}_3)_3$  using anhydrous  $\text{N}(\text{CH}_3)_3$  to create ion-exchange sites. Conventional and microwave heating were used to synthesize 2-EHMA cross-linked copolymers. These copolymers were tested as phase transfer catalysts for the hydrolysis of *p*-nitrophenyl alkanoates in fluorinated solvents.

The overall synthesis is shown in Scheme 2. All the dispersion polymerizations were performed in HFE-7200, an isomeric mixture of perfluorobutyl ethyl ethers. HFE-7200 is an inert solvent and has boiling point of 76 °C, making HFE-7200 more convenient for the polymerizations than HFE-7100, perfluorobutyl methyl ethers which has bp of 60 °C. HFE-7200 is also miscible with some organic solvents and can dissolve significant amounts of other organic compounds.

**Scheme 2**



All the monomers EHMA, VBC, DVB, and AIBN used for the dispersion polymerization are soluble in HFE-7200. As the polymerization proceeds, the growing polymer becomes immiscible in the HFE-7200 and separates as macroscopic particles. The polymerization of hydrocarbon monomers in the fluorinated solvent needs a stabilizer to keep the insoluble polymer particles dispersed. A stabilizer must be amphipathic (contain both polymer-philic segment with an affinity for the final polymer particle surface and solvent-soluble segment which extends into the continuous phase) to prevent coagulation of polymer particles. For a material to be an effective stabilizer in the fluorinated solvents it must contain hydrocarbon and fluorocarbon segments. For this purpose we have chosen commercially available fluoroalkyl methacrylates OFPM and PFDM as comonomers to try to stabilize the particles by forming steric stabilizing chains on the particle surface. An alternative steric stabilizer we used is the fluorinated homopolymer PPFOA<sup>28</sup> that has been successfully employed for the polymerizations in supercritical carbon dioxide, because of its low surface tension and low cohesive energy density.<sup>29</sup> PPFOA adsorbs on to the particle surface during the polymerization to stabilize the polymer particles. Three copolymers, containing by weight 74 % of 2-EHMA, 25 % of VBC, 1% of DVB as a cross-linker and 2 % of either OFPM or PFDM as comonomer to stabilize the particles as they formed were synthesized by conventional heating. All the co-monomer compositions and the polymerization results with yields are listed in Table 1. The % yield was calculated from the weights of copolymer obtained to weight of monomer mixture used for polymerization.

**Table 1. EHMA Dispersion Polymers<sup>a</sup>**

F-component	wt %	heating method	product	physical state	Yield (%)
None	-	oil bath	<b>1</b>	foam	96
OFPM	2	oil bath	<b>2</b>	foam	48
PFDM	2	oil bath	<b>3</b>	foam	53
PPFOA	10 <sup>b</sup>	oil bath	<b>4</b>	coagulum	-
PPFOA	10 <sup>b</sup>	microwave	<b>5</b>	stable colloid	58

<sup>a</sup> EHMA (72-74 wt %), VBC (25 wt%), and DVB (1 wt %). <sup>b</sup> Based on monomers.

The polymerization of 2-EHMA, VBC, and DVB with no fluoromonomer in HFE-7200 gave a foamy polymer (**1**). In order to obtain more stable colloids, the polymerizations were repeated with 5-10 % of OFPM and PFDM comonomers, but the polymerization mixtures still foamed. This might be due to poor copolymerization of EHMA with the fluorinated monomers. Since our initial methods of polymerization using 5-10 wt % fluorocomonomer as a stabilizer did not improve the stability of polymer colloids, we performed solution polymerization of EHMA and OFPM in CDCl<sub>3</sub> to determine the relative rates of consumption of the two monomers. Figure 1 shows the relative rates of consumption of EHMA and OFPM with time. Results on solution polymerization showed that OFPM was slightly more reactive than EHMA. After 10 h polymerization, a highly viscous copolymer solution in CDCl<sub>3</sub> was obtained, with no separate phase of fluoro homopolymer. These observations suggest a normal free radical copolymerization.

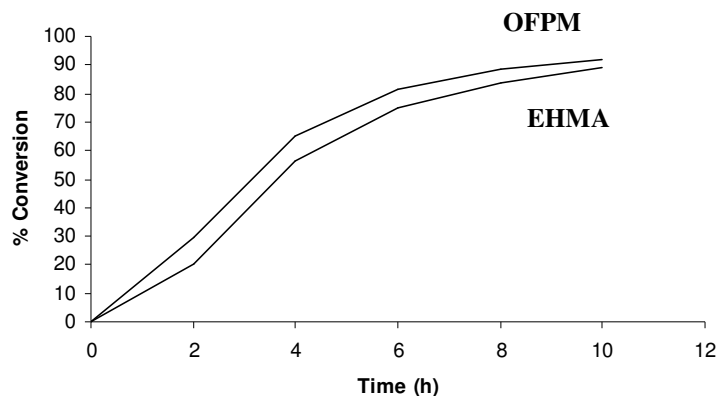


**Figure 1.** Monomer conversion vs. time for solution copolymerization of a 61/39 mol percent mixture of EHMA and OFPM.

All of the conventional polymerizations of 2-EHMA without or with 2 wt % of OFPM (**2**) and PFDM (**3**) at 65 °C started as homogeneous mixtures and turned cloudy due to nucleation of particles within 50-55 min. These dispersions were stable for 1-3 h during polymerization. EHMA copolymer dispersions were collected at 20 min intervals from the nucleation to the foamy stage to monitor the progress of the polymerization using  $^1\text{H-NMR}$  and dynamic light scattering (DLS). DLS studies showed increase in particle size from 300 nm to 570-590 nm during 1-3 h polymerization. NMR spectra of reaction mixture showed the relative increase in polymer peak height compared to that of monomer peaks. After 3 h, the particles coagulated and formed the foam. Solid copolymers were obtained by vacuum filtration and vacuum drying of the foam. Optical microscopic images revealed that the coagulated foams contained primary spherical particles about 1  $\mu\text{m}$  in diameter.

With the aim of obtaining more stable copolymers, all of the 2-EHMA polymerizations were repeated using a MARS<sup>TM</sup> CEM microwave reactor. Microwave

polymerization of 2-EHMA in the presence of PPFOA (10 wt %, Scheme 3) in HFE-7200 gave a stable dispersion (Table 1, sample 5) whereas conventional polymerization of 2-EHMA with 10 wt % poly(PFOA) gave coagulum. This method produced a stable dispersion of 1  $\mu\text{m}$  diameter spherical particles, as shown in the SEM image of Figure 2. Microwave polymerization of 2-EHMA with no fluoromonomer produced coagulum whereas polymerization was slow with 2 %, 5 %, and 10 % of OFPM and PFDM. Indeed, after 5 min of reaction time, the homogeneous solution turned cloudy due to nucleation of particles in microwave polymerizations, whilst nucleation took 55-60 min in conventional polymerizations. Polymerizations were carried to the point of no odor of residual monomers. Microwave polymerizations reached to the completion very fast within 4-5 h with 58-60 % yield than the conventionally-heated polymerizations of 24 h with 48-95 % yields. In case of solid polymers, the variations in the % yields were due to incomplete polymerization (% yields were calculated from the amount of polymer retrieved from the reaction flask after 24 h).

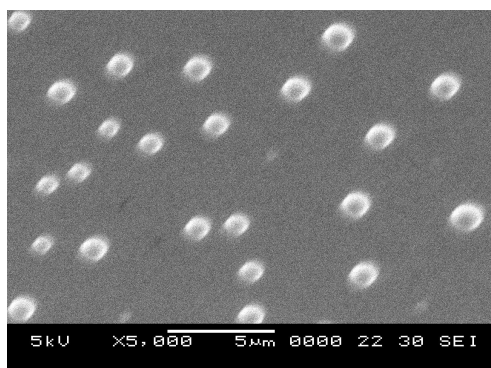
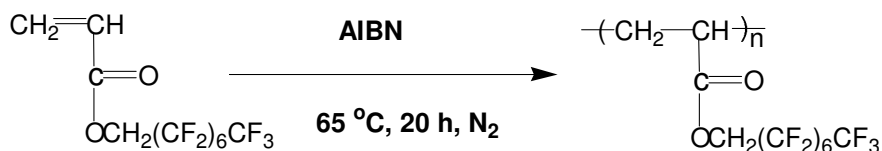


**Figure 2.** SEM image of cross-linked dispersion polymer particles (sample 5, Table 1).



### Scheme 3



**Conversion of VBC Units to Quaternary Ammonium Ions.** All the solid copolymers (**1**, **2**, and **3**) were treated with excess anhydrous trimethylamine in HFE-7200 under pressure at 60 °C to produce the quaternary ammonium ion polymers **6-8** reported in Table 2. The yields of quaternizations were in the range of 81-95 %. Optical microscopy (shown in Figure 3) studies revealed that coagulum consisted of primary particles of 1-2 μm along with some larger aggregates. The particle sizes are reported in Table 2.

**Table 2. Compositions of Quaternary Ammonium Ion Functionalized Polymers**

copolymer	product	yield (%)	diameter (μm)	Cl <sup>-</sup> (mmol/g)
<b>1</b>	<b>6<sup>a</sup></b>	81	2.08 ± 0.37 <sup>c</sup>	1.29
<b>2</b>	<b>7<sup>a</sup></b>	95	1.30 ± 0.19 <sup>c</sup>	1.55
<b>3</b>	<b>8<sup>a</sup></b>	93	1.44 ± 0.14 <sup>c</sup>	1.50
<b>5</b>	<b>9<sup>b</sup></b>	77	1.01 <sup>d</sup> , 1.04 <sup>e</sup>	1.14

<sup>a</sup>Conventional heating. <sup>b</sup>Microwave heating. <sup>c</sup>Optical microscopy. <sup>d</sup>DLS. <sup>e</sup>SEM.

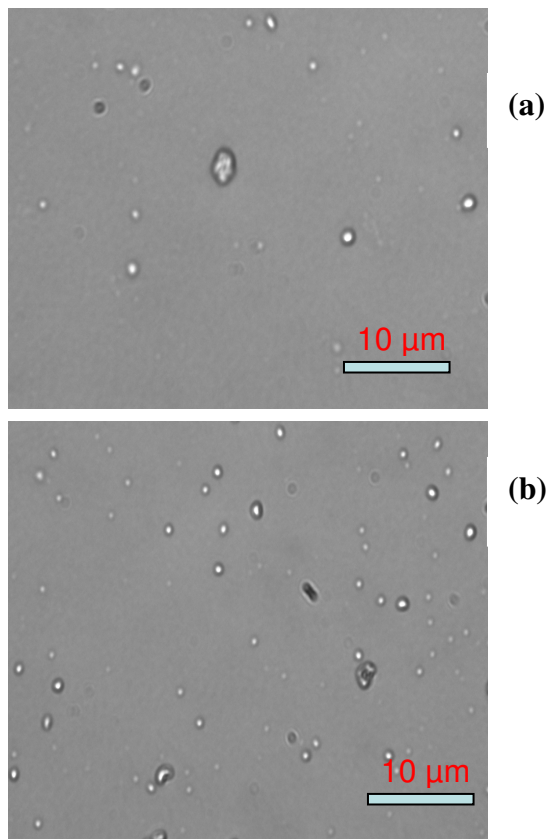


**Figure 3.** Optical microscopic images of quaternized solid polymers: (a) EHMA-OFPM-TMA (**7**), (b) EHMA-PFDM-TMA (**8**).

All of the foamy cross-linked 2-EHMA copolymers dispersed in HFE-7200 were freeze-dried and pulverized to fine powder to obtain IR spectra before and after quaternization (Figure 4). IR spectra of all solid polymers (**1**, **2**, and **3**) before quaternization had peaks corresponding to carbonyl ( $1718\text{-}1720\text{ cm}^{-1}$ ), C-O-C stretch ( $1200\text{-}1100\text{ cm}^{-1}$ ), C-H stretch ( $2980\text{-}2800\text{ cm}^{-1}$ ), C-F stretch (broad region at  $1300\text{-}1000\text{ cm}^{-1}$ ), and  $\text{-CH}_2\text{Cl}$  group at  $1262\text{ cm}^{-1}$ . IR spectra of all the solid polymers have no peak corresponding to  $\text{-CH}_2\text{Cl}$  group after quaternization. Further,  $\text{N}^+$  (mmol) units per gram of latex in these

solid polymers were determined by potentiometric titration with  $\text{AgNO}_3$  solution and a chloride selective electrode as illustrated by Figure 5. The results reported in Table 2 were almost same as that of theoretical value (1.6 mmol/g). Dried solid (10 mg) of the EHMA copolymer with OFPM (2) was analyzed for carbon, hydrogen and fluorine content. Elemental analysis proved that almost all the fluoromonomer used was present in the cross-linked EHMA copolymer.

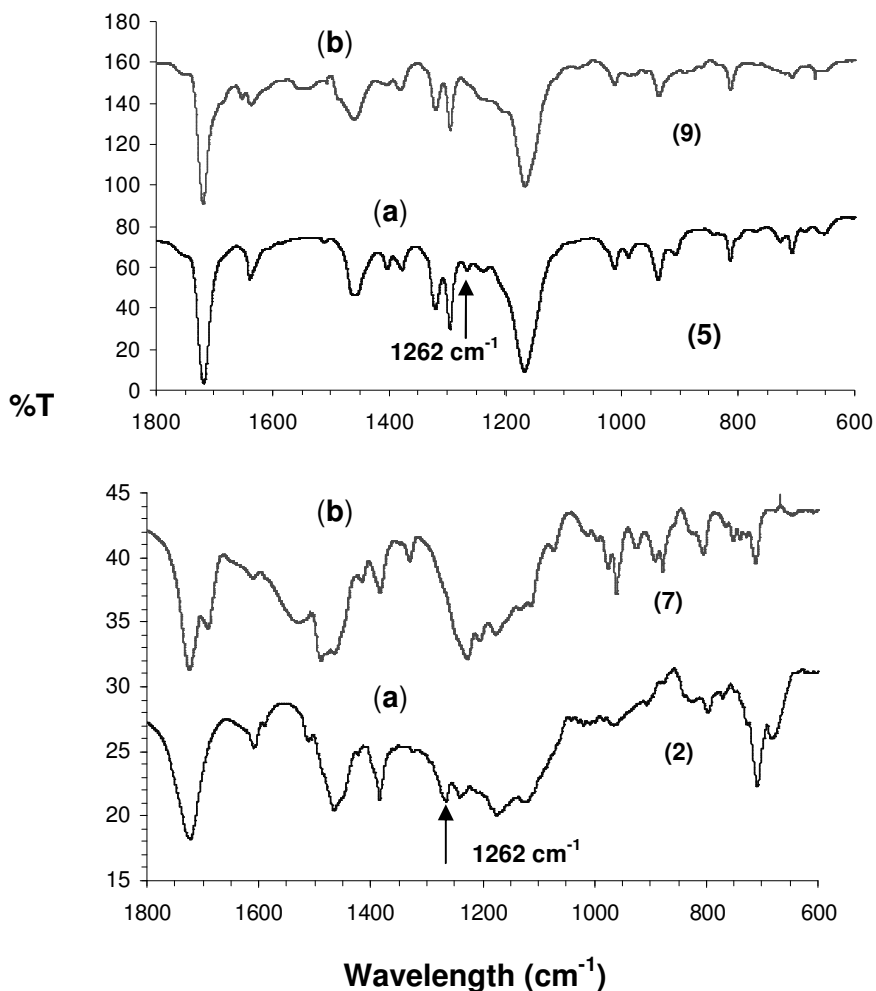


**Figure 4.** FT-IR spectra of 2-EHMA cross-linked copolymers by microwave (top) and conventional (bottom) polymerizations: (a) before quaternization, (b) after quaternization.

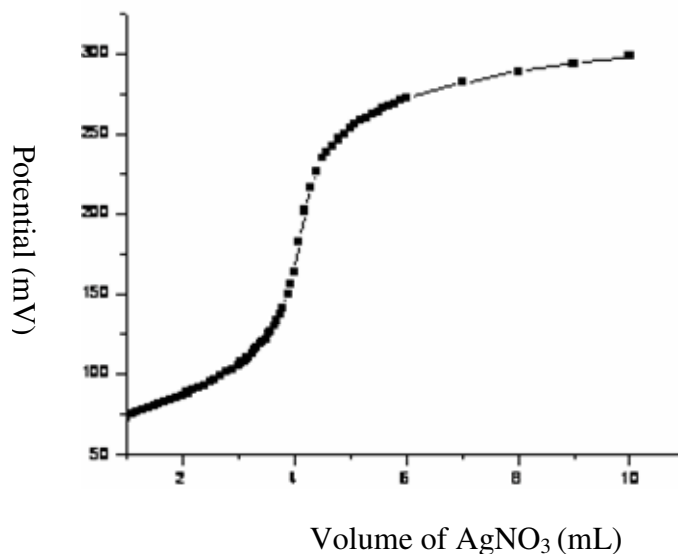


**Figure 5.** Potentiometric curve for quaternized copolymer **7** vs AgNO<sub>3</sub>.

Quaternization reactions of stable copolymer dispersion **5** in HFE-7200 with aqueous trimethylamine at 25 °C by stirring in a scintillation vial gave viscous polymer. Conventional heating of the stable dispersion with anhydrous trimethylamine at 60 °C for 48 h in a stainless steel reactor under pressure gave a two phase mixture consisting of brown oil and HFE-7200. Microwave heating of stable copolymer **5** with a 30-fold excess of anhydrous trimethylamine gave stable light yellow color quaternized polymer **9**. The IR spectra of polymer **5** showed the characteristic peak for –CH<sub>2</sub>Cl group at 1262 cm<sup>-1</sup> and no such peak in the quaternized polymer **9** (Figure 4). Particle size diameters measured under dry and swollen conditions by SEM (Figure 2) and dynamic light scattering were about the same and were on the order of 1 μm. Further, N<sup>+</sup> (mmol) units per gram of latex determined by potentiometric titration with a chloride selective electrode for this stable dispersion **9** was 1.14 mmol/g (Table 2, Figure 5). The

microwave method gave more stable copolymer and more stable quaternized polymer compared to conventional heating.

**Hydrolysis of PNPH by Solid (6, 7, and 8) and Stable (9) Copolymers.** Four different copolymers (6, 7, 8, and 9) were tested as phase transfer catalysts for hydrolysis of *p*-nitrophenyl hexanoate (PNPH). The copolymers differed in the type of stabilizer, either 1H,1H,5H-octafluoropentyl methacrylate (OFPM), 1H,1H,2H,2H-perfluorodecyl methacrylate (PFDM), or poly (perfluorooctyl acrylate) (PPFOA). The solid copolymers ((6, 7, and 8) and the liquid copolymer dispersion 9) were analyzed by optical microscopy, dynamic light scattering (DLS), and scanning electron microscopy (SEM) in order to determine the sizes under dry and swollen conditions.

**Hydrolysis of PNPH by Copolymers (6, 7, and 8) in Cl<sup>-</sup> Form in NaOH Solution.** All the solid copolymers in Cl<sup>-</sup> form (6, 7, and 8) and in OH<sup>-</sup> form (10, 11, and 12) (Table 3) were tested for the PNPH hydrolysis at pH 9 and at room temperature. Initial studies on the PNPH hydrolysis by 1 mg of solid copolymer 7 in 2.995 mL of 0.01 M NaOH solution and 5  $\mu$ L of 2.5 mM PNPH in acetonitrile showed that 76% of PNPO<sup>-</sup> got into copolymer particles, which was calculated as follows. The concentration of PNPO<sup>-</sup> in the aqueous phase was calculated from the absorbance at 400 nm, the molar extinction coefficient  $\epsilon = 21,440$  of the PNPO<sup>-</sup>, and  $Abs = \epsilon bc$  ( $b$  is path length (1 cm) and  $c$  is the molar concentration), and the remainder was the fraction in the particle phase. In this experiment, the particles were floating and the aqueous phase turned yellow due to PNPO<sup>-</sup>. Similar hydrolysis was performed using 2 mL of 0.01 M NaOH, 2 mL of HFE-7200, and the polymer particles. After 20 min equilibration,  $3.1 \times 10^{-6}$  mmol of PNPH/(CH<sub>3</sub>)<sub>2</sub>CHOH was added to the particles, and the PNPO<sup>-</sup> absorbance was

monitored by UV-Vis. In this triphase system, the particles stayed at the interphase between water and HFE-7200.

In PNPB hydrolysis by solid copolymer **7** in Cl<sup>-</sup> form in basic solution that only 76 % of PNPB was hydrolyzed. It is hard to measure the PNPO<sup>-</sup> absorbance and % conversion of PNPB in case of mixture of solid polymers, NaOH, and HFE-7200 due to noise caused by the zig-zag (Brownian) motion of the particles. Also the particles stuck on the walls of the cuvette.

**Table 3. Concentrations of Cl<sup>-</sup>, OH<sup>-</sup>, and Swelling Ratios for Solid Copolymers**

Solid polymer in Cl <sup>-</sup> form	Solid polymer in OH <sup>-</sup> form	particle size (μm)	Swelling ratio	Cl <sup>-</sup> (mmol/g) of polymers <b>6-8</b>	OH <sup>-</sup> (mmol/g) of polymers <b>10-12</b>
<b>6</b>	<b>10</b>	2.08 ± .37 <sup>a</sup>	3.14	1.29	0.30
<b>7</b>	<b>11</b>	1.30 ± .19 <sup>a</sup>	3.05	1.60	0.40
<b>8</b>	<b>12</b>	1.44 ± .14 <sup>b</sup>	2.00	1.50	0.30

<sup>a</sup>Optical microscopy. <sup>b</sup>SEM. Swelling ratio = (swollen volume)/ (dry volume)

**Hydrolysis of PNPB by Copolymers (6, 7, and 8) in Cl<sup>-</sup> Form in HFE-7200.**

We tried to repeat the PNPB hydrolysis in HFE-7200 by shaking of two phases rather than stirring. Physical mixing of two phases (particles/HFE) by shaking caused the particles to float on the HFE-phase rather than sticking to the walls of the cuvette. The shaking method increased the intensity of light reaching the detector by minimizing the particle scattering. This was a two step method. In step 1 the particles containing 16 μmol

of  $N^+$  in chloride form were equilibrated with 3 mL of HFE-7200 and  $16.7 \times 10^{-6}$  mmol of PNPH, and the UV-Vis spectrum of HFE phase showed the preferential partitioning of PNPH in HFE. In step 2 PNPH absorbed particles were treated with  $5 \times 10^{-4}$  mol of aqueous  $NaNO_3$  to displace the  $PNPO^-$  from the particles. The UV-Vis spectrum of the aqueous phase showed the peak corresponding to PNPH at 290 nm, not  $PNPO^-$  at 410 nm, which indicates that the hydrolysis of PNPH did not occur. PNPH did not react because the  $Cl^-$  form of particles has impermeable fluoropolymer on their surface.

#### **Hydrolysis of PNPH by Copolymers (10, 11, 12) in $OH^-$ Form in HFE-7200.**

We decided to do the rest of the hydrolysis reactions with the  $OH^-$  form of particles since the  $Cl^-$  form of particles did not absorb PNPH. Several solvents and solvent mixtures ( $CH_3OH$ ,  $CH_3CH_2OH$ ,  $H_2O$ , DMF, THF, THF/DMF (1:1), THF/ $H_2O$  (1:1), THF/ $NaOH$  (5:1),  $CH_3OH/THF$  (1:9),  $(CH_3)_3CHOH/THF$  (1:9)), different mixing times, and with/without stirring were used to improve the incorporation of  $OH^-$  into polymer particles. In all these methods the concentration of  $OH^-$  found in the particles was 2-3  $\mu mol$  out of the total 16  $\mu mol$  which was equal to 12.5 %- 19 % of  $OH^-$ . These values were obtained by washing the particles in  $OH^-$  form with 1M  $NaNO_3$  for 2-3 times to displace  $OH^-$  by  $NO_3^-$  and titrating the collected  $OH^-$  against the standard 0.01 M HCl with phenolphthalein as an indicator. The end point was pink to colorless. The particles floated on all of the solvents used for wetting and also during the ion-exchange of  $Cl^-$  in particles by  $OH^-$  using  $NaOH$ . This observation reveals that excess air trapped in particles might have prevented the incorporation of  $OH^-$  into the particles. We attempted to evacuate the particles in THF to get rid of air in the particles. THF was chosen for wetting the particles since 75% of polymer is EHMA and it is a good solvent to

PolyEHMA. Finally, the Cl<sup>-</sup> particles wetted with THF were ion-exchanged by OH<sup>-</sup> and used for hydrolysis of PNP<sup>+</sup>H ester. Concentrations of Cl<sup>-</sup>, OH<sup>-</sup>, and wet ratios for all quaternary ammonium ion latexes (**6**, **7**, and **8**) are reported in Table 3. Swelling ratios were obtained by the weight ratios of the OH<sup>-</sup> form of wet polymer particles to the dry particles.

In all of the PNP<sup>+</sup>H hydrolysis experiments, no hydrolysis was initiated by dry particles (**6-8**) since no PNPO<sup>-</sup> peak was observed at 400-410 nm and the hydrolysis did not go to completion using wet particles (**10-12**). The particles in OH<sup>-</sup> form do contain the considerable amounts of Cl<sup>-</sup> (80 %) after ion-exchange treatment. The % PNP<sup>+</sup>H hydrolyzed by wet particles was calculated by measuring PNP<sup>+</sup>H absorbance in HFE phase and calculating [PNP<sup>+</sup>H] using Abs = ε bc and the ε of PNP<sup>+</sup>H (5488). Though we used 100-1000/1 fold mole ratio of N<sup>+</sup>/ PNP<sup>+</sup>H (Table 4), the % PNP<sup>+</sup>H hydrolyzed by wet solid copolymers (**10**, **11**, and **12**) was 6-10 %. In PNP<sup>+</sup>H hydrolysis by dry solid particles in borate buffer solution at pH 9.38 and at temperature 30 ± 1°C, the PNP<sup>+</sup>H ester is trapped inside the particles.

**Table 4. Hydrolysis of PNP<sup>+</sup>H by Wet Solid Copolymers**

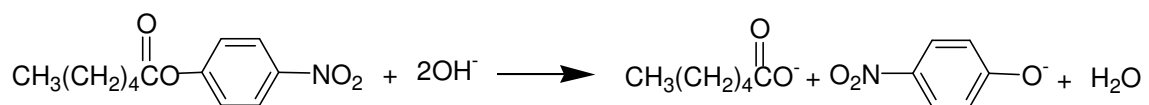
solid polymer <sup>a</sup>	% PNP <sup>+</sup> H in HFE phase	% PNP <sup>+</sup> H hydrolyzed
<b>10</b>	90.2	9.8
<b>11</b>	93.5	6.5
<b>12</b>	92.3	7.7

<sup>a</sup> solid polymer (40 mg, 6.4x10<sup>-2</sup> mmol of N<sup>+</sup>), HFE-7200 (3 mL), and PNP<sup>+</sup>H (1.67x10<sup>-5</sup> mmol)



**Hydrolysis of PNPB by Stable Copolymer (9) in Cl<sup>-</sup> Form in HFE-7200 and Borate Buffer Mixture.** To test catalytic activities of the stable polymer (9) particles, we measured the rates of basic hydrolysis of *p*-nitrophenyl hexanoate (PNPB) (shown in Scheme 4) in pH 9.4 borate buffer solution with the quaternary ammonium sites in a greater than 5-10 fold excess over substrate. PNPB is hydrophobic but completely soluble in HFE dispersion at the concentration needed for kinetic measurements. Initially hydrolysis reactions were carried out in a polystyrene cuvette without stirring using 4-40  $\mu\text{L}$  of polymer particles in HFE-7200 (0.16 mg -1.6 mg,  $6.13 \times 10^{-6}$  - $6.13 \times 10^{-4}$  mmol of N<sup>+</sup>) and 30  $\mu\text{L}$  of 2.5 mM ( $37.5 \times 10^{-6}$  mmol) PNPB/CH<sub>3</sub>CN in 2.5-3.0 mL of borate buffer of pH 9.38. A control experiment was also performed without particles to know the effect of polymer particles on the rate of hydrolysis. The rate of PNPB ester hydrolysis decreased with increase in polymer particle concentration and is shown in Figure 6. This might be due to slow ion-exchange of Cl<sup>-</sup> by OH<sup>-</sup>. In absence of stirring, most of the active sites located within the polymer particle may not come in contact with buffer for the ion-exchange of Cl<sup>-</sup> in particles by OH<sup>-</sup>. Decrease in reaction rates are due to less number of OH<sup>-</sup> sites on particle surface to hydrolyze PNPB.

**Scheme 4**



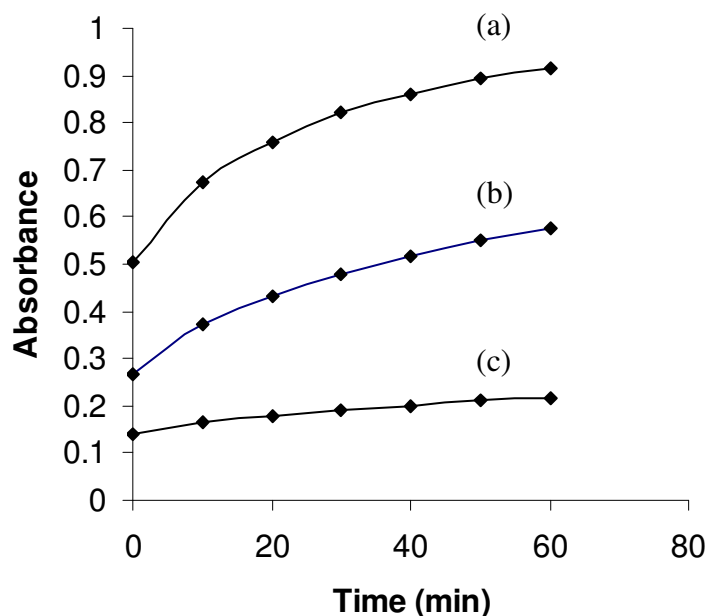


**Figure 6.** Absorbance of  $\text{PNPO}^-$  from hydrolysis of PNPH in borate buffer/HFE-7200 mixtures without stirring at 25 °C: (a) with no polymer particles, (b) 0.16 mg of particles, (c) 1.6 mg of particles

In order to increase the rate of hydrolysis, experiments were performed in a 50 mL round bottom flask with magnetic stirring and at  $30 \pm 1^\circ\text{C}$  using 0-100  $\mu\text{L}$  of polymer particles (0-4 mg,  $0-46 \times 10^{-4}$  mmol of  $\text{N}^+$ ) in HFE-7200, 368  $\mu\text{L}$  of 2.5 mM PNPH ( $0.92 \times 10^{-4}$  mmol), and 0.02 M of pH 9.4 borate buffer. One mL of HFE-7200 was added to reaction medium to keep the particles well dispersed in borate buffer during the progress of reaction. This experiment was a two stage process. The schematic diagram is shown in Figure 7. In the first stage 50-100  $\mu\text{L}$  (2-4 mg) of polymer particles in HFE dispersion, 1 mL of HFE-7200, and 9 mL of 0.02 M borate buffer were stirred magnetically for 60 min at  $30 \pm 1^\circ\text{C}$  to exchange the  $\text{Cl}^-$  of the particles with  $\text{OH}^-$  of the

buffer. In the second stage when 368  $\mu\text{L}$  of PNPH in  $\text{CH}_3\text{CN}$  ( $9.2 \times 10^{-5}$  mmol) was added directly to the HFE phase by micro pipette, the HFE phase turned yellow immediately due to the presence of  $\text{PNPO}^-$  in the particles. The triphase mixture containing the polymer particles, HFE, and aqueous buffer was stirred magnetically for an hour to monitor the transport of  $\text{PNPO}^-$  from the particles to the aqueous phase. In 2-5 min, the whole mixture turned bright yellow and cloudy due to dispersion of visible HFE droplets in water like oil in water. The color of the HFE phase changes from bright yellow to pale yellow within 40-45 min and almost colorless at the end due to decrease in concentration of  $\text{PNPO}^-$  in the particles. Stirring was stopped every 2 min to record the absorbance of  $\text{PNPO}^-$  in the aqueous phase. The HFE phase separates and settles to the bottom of the flask rapidly. The yellow aqueous phase of 100-150  $\mu\text{L}$  was transferred to a 1cm path length cell thermostated at  $30 \pm 1$   $^\circ\text{C}$  to record the UV-Vis spectrum of  $\text{PNPO}^-$ . The absorbance of  $\text{PNPO}^-$  in the water phase increased with time and attained the maximum value of 2.2 in an hour with almost 100% conversion. After one hour the HFE phase was almost colorless which indicates the completion of hydrolysis. The time required for half of the transfer ( $t_{1/2}$ ) of  $\text{PNPO}^-$  to the aqueous phase with polymer particles was 5.0-5.5 min and with no polymer particles was 8.8-9.0 min (shown in Figure 8). All experiments on PNPH had half-lives for transfer of  $\text{PNPO}^-$  to the aqueous phase within the range of 5.5-10 min as shown in Table 5. With no polymer particles (entries 1 and 4, Table 5), the  $\text{PNPO}^-$  transfer was slower.  $\text{PNPO}^-$  transfer went faster in the presence of 2 mg of polymer particles (entries 1, 2, 4, and 5, Table 5) than in the absence of polymer particles. The rate decreased with increase in amount of polymer particles (4 mg) (entries 3 and 6, Table 5). Increase in pre-mixing time of particles, HFE, and borate buffer prior to the

addition of PNPB, increased the rate of transfer of PNPO<sup>-</sup> to the water phase (shown in Table 6). The effect of pre-mixing time on  $t_{1/2}$  by stirring the mixture of HFE-7200, particles, and buffer solution before the addition of PNPB using 100  $\mu$ L of polymer particles is shown in Table 6. Rates were increased with increase in pre-mixing time, probably due to the ion-exchange of Cl<sup>-</sup> in the fluorinated phase particles by OH<sup>-</sup> in the aqueous phase. That is, longer premixing time gives higher concentration of OH<sup>-</sup> in the particles and thereby faster production of PNPO<sup>-</sup> from PNPB, and faster transport of PNPO<sup>-</sup> into the aqueous phase.

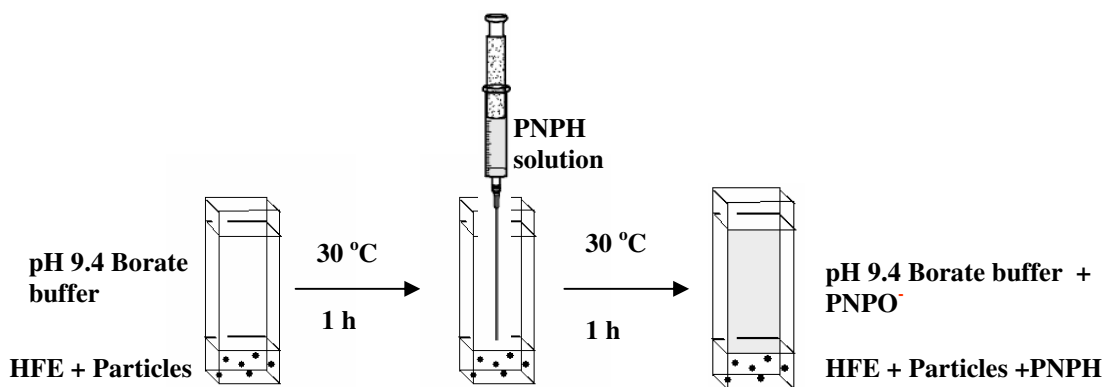


**Figure 7.** Hydrolysis of PNPB in a 3-phase mixture consisting of polymer particles, HFE-7200, and pH 9.4 borate buffer.

**Table 6. Decrease in  $t_{1/2}$  with Increase in Contact Time/ Stirring Before Adding PNPB<sup>a</sup>**

Stirring time (min)	10	30	60
$t_{1/2}$ (min)	22	18	6.9

<sup>a</sup> For conditions see Table 5.

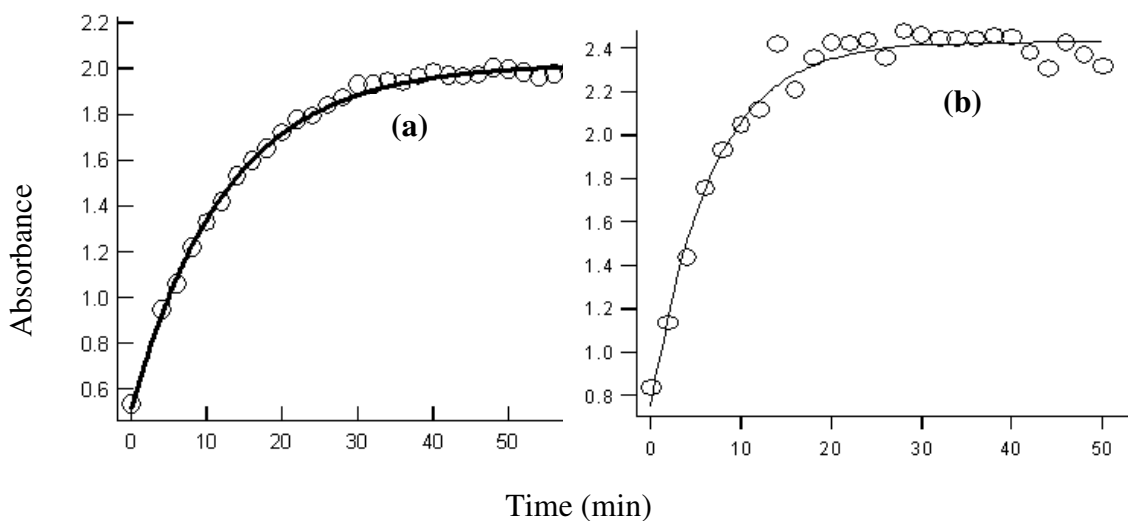


**Figure 8.** Appearance of  $\text{PNPO}^-$  absorption at 400 nm in the aqueous phase: (a) with no particles, (b) with 2 mg (50  $\mu\text{L}$ ) of particles. Conditions are in Table 5.

**Table 5. Hydrolysis of PNP<sup>H</sup> by Stable Polymer Particles**

Experiment <sup>a</sup>	Weight of polymer particles (mg)	$[\text{N}^+]$ (mmol/mL)	$t_{1/2}$ (obs) min	$t_{1/2}$ (cal) min
1	---	---	8.80	9.00
2	2	$2.3 \times 10^{-4}$	4.88	4.59
3	4	$4.6 \times 10^{-4}$	5.33	5.79
4	---	---	8.60	8.90
5	2	$2.3 \times 10^{-4}$	5.47	5.25
6	4	$4.6 \times 10^{-4}$	6.90	6.90

<sup>a</sup> PNP<sup>H</sup> (368  $\mu\text{L}$  of 2.5 mM,  $9.2 \times 10^{-5}$  mmol/mL), borate buffer (9.0 mL of 0.02 M, pH 9.38), and HFE-7200 (1.0 mL)

The half-life  $t_{1/2}$  (cal) was calculated using  $k = (1/t) \ln(A_{\infty}-A_0)/(A_t-A_0)$  and  $t_{1/2} = \ln(2)/k$ , and  $t_{1/2}$  (obs) was calculated using Igor pro 6.1 version software. Similar experiments that were performed in a quartz cuvette with or without shaking and with magnetic stirring did not give reproducible results because of mixing problems.

## Discussion

Microwave heated polymerizations proceeded faster with shorter nucleation times compared to that of conventional heating methods. Increases in reaction rates by microwave irradiation in most cases are due to instantaneous and rapid heating which results in a uniform heating of reaction mixture and also reverse thermal effect (heating starts from the interior of the material).<sup>30-32</sup> In general, microwave absorption occurs when one or more of the reaction components possesses either a dipole moment or charge to align with the electric field of the microwave. The dipoles of molecules constantly try to realign with the oscillating electric field. This continual re-orientation of molecule produces heat and is called as dipolar heating. Solvents with high dielectric constant such as water, ethanol, and DMF, absorb much more microwave energy than nonpolar solvents such as hydrocarbons. In our dispersion polymerizations the fluorinated solvent (HFE-7200) might have a greater dipole moment than OFPM and PFDM to absorb high microwave energy. Moreover HFE-7200 was the major component of the mixture. The microwave heated polymerization of 2-EHMA, VBC, DVB, and PPOFA in HFE-7200 proceeded faster with shorter nucleation times because of more rapid heating of the reaction mixture. Internal rapid heating is known for raising the temperature of the

reaction medium to higher than the temperature recorded by the fiber optic sensor.<sup>32</sup> The fiber optic sensor was positioned at the center of the control vessel. These high temperatures increase the rate of initiator decomposition to radicals which leads to shorter nucleation times.

The fluoro homopolymer (PPFOA) stabilizer used for the polymerization has no methyl substituent on the backbone and is more flexible than the copolymers of EHMA and the comonomers (OFPM and PFDM). This flexibility might have helped the PPFOA to adsorb on the growing 2-EHMA backbone during the polymerization to keep the polymer particles dispersed in HFE-7200 and to form stable dispersions.

Microwave polymerizations gave stable dispersions whereas conventional polymerizations gave coagulated polymers. Early coagulation might happen because of non-uniform heat transfer from the oil bath to the reaction medium, and the evaporation of solvent. In the conventional heating, molecular collisions and the energy of the system depends on diffusive heat transfer from the oil bath to the walls of the flask and to the reaction mixture, whereas in microwave heating the heat from a microwave radiation transferred directly to the molecules and the excess heat is transferred to walls of the vessel. Most efficient heat transfer in microwave reactors makes the polymerizations proceed faster than by the conventional heating methods. In addition, functional group transformation of the dispersion particles from chloromethyl or VBC groups to quaternary ammonium ions using anhydrous trimethylamine also gave stable dispersions by microwave heating. Possibly the quaternary ammonium chloride ion pairs absorb more microwave radiation than the starting EHMA-VBC copolymer since ionic liquids

are good solvents for microwave heating.<sup>33</sup> These quaternized dispersions contained discrete particles of diameter 1  $\mu\text{m}$ .

All three cross-linked quaternized solid copolymers **6**, **7**, and **8** and the stable cross-linked copolymer **9** were tested as phase transfer catalysts for the hydrolysis of *p*-nitrophenyl hexanoate (PNPH) in HFE-7200. Hydrolysis experiments were performed in a cuvette containing a 3 phase mixture of particles, HFE-7200 and borate buffer at pH 9.4 with magnetic stirring at 25 °C. Rates of hydrolysis decreased with the 10 fold increase in concentration of solid polymer particles. The % PNPH hydrolyzed was very small i.e. 6.5%-9.8% compared to that of amount of PNPH in HFE phase. UV-Vis spectrum of the HFE phase showed the peak corresponding to PNPH at 290 nm. This is possibly because of the particles in OH<sup>-</sup> form contained ~ 80% of Cl<sup>-</sup> after the evacuation of the particles in THF and the ion-exchange by 1 M NaOH. Attempts to improve the incorporation of OH<sup>-</sup> into the Cl<sup>-</sup> form of particles using various solvents were unsuccessful. This might be due to the presence of an impermeable fluoropolymer layer on the particle surface. The fluoro comonomer used for stabilization of polymer particles during the polymerization coats onto the particle surface and makes the particle surface impermeable not only for OH<sup>-</sup> during the ion-exchange but also for PNPO<sup>-</sup> during the hydrolysis. This explains the preferable partitioning of PNPH into HFE phase rather than into particles during the hydrolysis shown in Table 4. Alternatively, PNPH ester hydrolysis was carried out using the stable polymer particles dispersed in HFE-7200 and borate buffer. Rates of hydrolysis were slow without stirring and with a 10 fold increase in polymer particles due to slow ion-exchange of Cl<sup>-</sup> by OH<sup>-</sup> (Figure 6). The polymer particles are cross-linked and contain ionic sites inside the particles as well as on the surface. If the polymer



particles are not swollen enough, the number of ( $\text{Cl}^-$ ) ionic sites that come into contact with borate buffer for  $\text{OH}^-$  exchange will be less, and the PNP $\text{H}$  will hydrolyze less efficiently.

Hydrolysis reactions were repeated with 2-4 mg of stable particles using a round bottom flask and a mixture of 9.0 mL of borate buffer and 1.0 mL of HFE-7200 as a reaction medium to provide more room for the particles while stirring and also to keep ion-exchange particles well dispersed during the hydrolysis. Reaction rates were doubled relative to the control experiment which lacked polymer latex particles (Figure 8). Faster rates of hydrolysis in a three phase mixture containing particles, HFE, and borate buffer (Figure 9) can be explained like this:<sup>34-36</sup> 1) Polymer particles transport  $\text{OH}^-$  ion from the buffer phase to HFE-7200 for the ion-exchange of  $\text{Cl}^-$  in particles by  $\text{OH}^-$ . Pre-mixing the mixture of HFE phase containing 2-4 mg of particles and buffer by stirring for 60 min prior to the addition of PNP $\text{H}$  facilitated the  $\text{Cl}^-$  exchange by  $\text{OH}^-$  in the particles. 2) PNP $\text{H}$  diffuses from the bulk HFE phase to the polymer particle surface and then to active  $\text{N}^+$  ion sites of polymer particles. Constant stirring of mixture containing particles in  $\text{OH}^-$  form in HFE dispersion and PNP $\text{H}$  in HFE phase will facilitate this. 3) Reaction of PNP $\text{H}$  with  $\text{OH}^-$  occurs in the particle phase. After the addition of PNP $\text{H}$ , the HFE phase turned yellow very quickly, which reveals that  $\text{PNPO}^-$  was in the particle phase. Our control experiment on addition of PNP $\text{H}$  to water and HFE also showed the partitioning of PNP $\text{H}$  in the HFE. 4) Diffusion of the product  $\text{PNPO}^-$  to the surface of the polymer particles and its mass transfer to the buffer phase. The change in color of HFE phase from bright yellow to pale yellow and almost colorless at the end proves the transport of  $\text{PNPO}^-$  from the particles in the HFE phase to the buffer phase. The change

in color of HFE phase with time will give insight that the bulk amounts of PNP<sup>H</sup> and OH<sup>-</sup> are in the particle phase in HFE. UV-Vis spectra of the water phase showed that the absorbance of PNPO<sup>-</sup> increased with time and reached to 100% conversion in an hour. Though the reaction took place in the particle phase in HFE, all the products (PNPO<sup>-</sup>, CH<sub>3</sub>(CH<sub>2</sub>)<sub>4</sub>COO<sup>-</sup>, and H<sub>2</sub>O) were transported to the buffer phase because of their ionic nature. In summary, the ion exchange of Cl<sup>-</sup> by OH<sup>-</sup> and consistent stirring were vital for the hydrolysis of PNP<sup>H</sup> in HFE/ buffer mixtures to reach 100% conversion. Faster stirring aids mass transfer of PNP<sup>H</sup> into the polymer particles and reaction occurs only at interior active sites. Increase in premixing time (10-60 min) of particles and buffer increased the ion exchange of Cl<sup>-</sup> by OH<sup>-</sup> and decreased the  $t_{1/2}$  values from 22 min to 6.9 min. Rate of PNP<sup>H</sup> hydrolysis by 4 mg of particles is rather slow compared to that of 2 mg of particles. Maximum pre-mixing time tried for the hydrolysis of 2-4 mg of particles is 60 min. Pre-mixing time of more than an hour is needed to increase the ion exchange of Cl<sup>-</sup> by OH<sup>-</sup> in case of PNP<sup>H</sup> hydrolysis with increased particle concentration. The polymer particles are cross-linked EHMA quaternary ammonium salts and can be referred to as ion-exchange resins. The hydrolysis of the PNP<sup>H</sup> by ion-exchange resins was mainly due to mass transfer of the PNP<sup>H</sup> to the active site in the polymer particle and to the transfer of PNPO<sup>-</sup> to aqueous phase.<sup>7</sup> Polymer particles increase the mass transfer of PNPO<sup>-</sup> bound quaternary ammonium ions from HFE phase to buffer phase with increase in stirring time due to their large surface area with large number of ionic sites. This might lead to an increase in reaction rates.

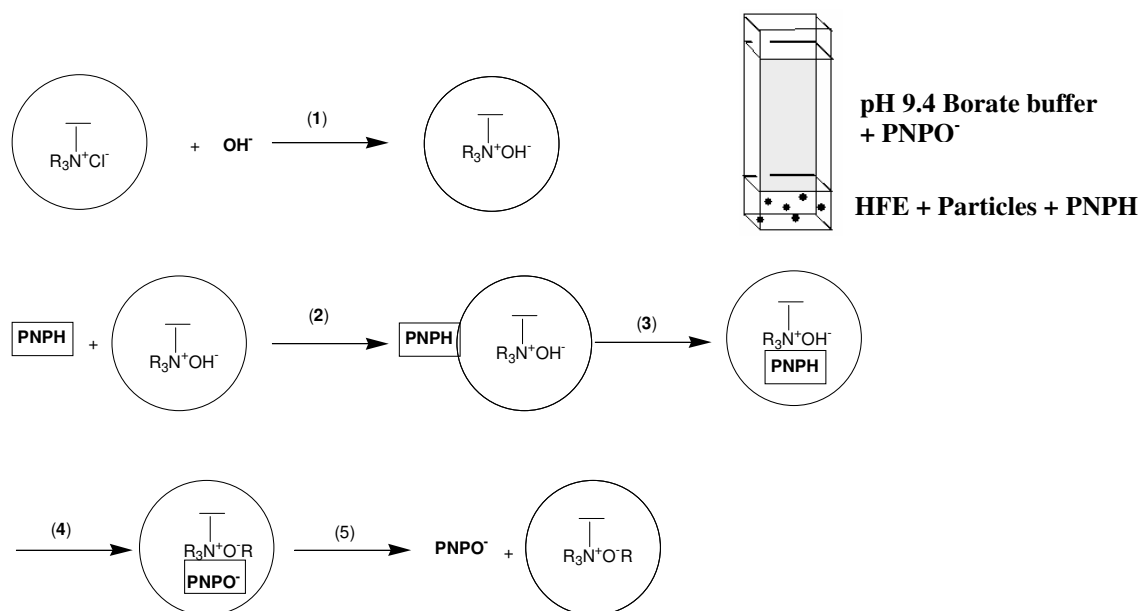


**Figure 9.** Mechanism for the hydrolysis of PNPH in a polymer supported phase transfer catalysis.

Our research work on synthesis of quaternized cross-linked copolymers and functional group conversions in fluorinated solvents by dispersion polymerization using microwave heating proved that the preparation of stable dispersions of copolymers containing EHMA, VBC, and DVB in HFE-7200 is fast and simple. Unfortunately, the quaternized poly(ethylhexyl methacrylate) latexes are not effective phase transfer catalytic media for the hydrolysis of carboxylate esters. The primary factor responsible for the limited catalytic activity of these particles in a three phase mixture of particles, HFE-7200 and borate buffer is the mass transfer limitation of  $\text{OH}^-$  from the aqueous phase into the particles of  $\text{Cl}^-$  form in HFE phase. Our preliminary studies on hydrolysis of carboxylate esters by catalytic polymer particles has shown that the reaction rate has increased by factor of 2 with increase in premixing time of particles and buffer.

In order to achieve our target of the decontamination of simulants of CW agents from contaminated electronic equipment in fluorinated solvent by polymer particles, the polymer particles should be made on a large scale, and the hydrolysis experiments should be performed using mechanical stirring to provide sufficient mixing which might increase the rate of mass transfer of  $\text{OH}^-$  from the buffer into the particles in HFE phase. Similarly, the particles in  $\text{Cl}^-$  form can be transformed to  $\text{OH}^-$  form by treating the particles with strong base or using commercially available ion-exchange resins prior to the hydrolysis. Alternatively, the cross-linked copolymer particles using EHMA, VBC, and DVB could be synthesized in aqueous media and this mixture could be stirred with fluorinated solvent containing the simulants of chemical warfare agents for decontamination studies.

### Summary

Ethylhexyl methacrylate (EHMA) cross-linked copolymers were synthesized by conventional and microwave dispersion polymerizations in nonafluorobutyl ethyl ether (HFE-7200). Four different copolymers of EHMA, vinylbenzyl chloride (VBC), and divinylbenzene (DVB) were made using fluoromonomer 1H,1H,5H-octafluoropentyl methacrylate (OFPM), or 1H,1H,2H,2H-perfluorodecyl methacrylate (PFDM), or poly(1,1-dihydroperfluorooctyl acrylate) (poly(PFOA) stabilizer in HFE-7200). The  $-\text{CH}_2\text{Cl}$  groups of the polymers were converted to  $-\text{CH}_2\text{N}^+(\text{CH}_3)_3\text{Cl}^-$  to create ion-exchange sites using anhydrous trimethylamine. These copolymers were characterized by FTIR, DLS and SEM analyses. The copolymer particles were spherical and 1  $\mu\text{m}$  in

diameter.  $N^+$  (mmol) units per gram of stable latex determined by potentiometric titration with a chloride selective electrode were 1.14 mmol/g. These new hydrophobic quaternized EHMA copolymers make phase transfer catalysts. The rates of hydrolysis of *p*-nitrophenyl hexanoate (PNPH) ester were measured in basic borate buffer and HFE-7200 mixtures at  $30 \pm 1^\circ\text{C}$  in the presence of 2-4 mg of quaternary ammonium ion exchange latex particles and without particles. PNPH hydrolysis was faster in polymer latex particles in pH 9.4 borate buffer at  $30 \pm 1^\circ\text{C}$  relative to control experiments which lacked polymer latex.

## Experimental

**Materials.** 2-Ethylhexyl methacrylate (2-EHMA, 98 %), was from Aldrich Co., divinylbenzene (DVB, 55-60 %, *m/p* isomeric mixture) was from Polysciences, chloromethylstyrene (VBC, 96 %, *m/p* isomeric mixture) was from Scientific Polymer Products, Inc., and cyclohexane- $d_{12}$  (98 %) was from Cambridge Isotope Laboratories, Inc. The isomeric mixture of nonafluorobutyl ethyl ethers (HFE-7200) from 3M Novec Engineered Fluids. HFE-7200 was purified using simple distillation at  $70^\circ\text{C}$ . The first and the last fractions (10 % each) were discarded for purity purposes. 1H,1H,5H-Octafluoropentyl methacrylate (OFPM), 1H,1H,2H,2H-perfluorodecyl methacrylate (PFDM, 97 %), 2H,3H-perfluoropentane (PFP, 98 %), 1H,1H-perfluorooctyl acrylate (PFOA), and (heptadecafluoro-1,1,2,2-tetrahydrodecyl) dimethylchlorosilane (HDF) were from Synquest Labs., Inc. Phenolic inhibitor was removed from the monomers by a column of basic alumina. Aluminum oxide ( $\text{Al}_2\text{O}_3$ , activated, basic, ~ 150 mesh,  $58 \text{ \AA}$ ),

dichloromethane (CH<sub>2</sub>Cl<sub>2</sub>, 98 %), chloroform (CDCl<sub>3</sub>, 99.9 % D), and anhydrous trimethylamine (N(CH<sub>3</sub>)<sub>3</sub>, 99 %) from Aldrich Co. were used as received. 2,2'-Azobis(2-methylpropionitrile) (98 %, AIBN) was recrystallized from ethanol. Nitrogen purged, deionized water was used for all polymerizations. Poly(perfluorooctyl acrylate) (PPFOA) was synthesized by a literature method.<sup>28</sup> *p*-Nitrophenyl acetate (TCI America) was used as a 2.5 mM solution in acetonitrile.

**Instrumentation.** Potentiometric titrations were carried out with an Orion combination chloride electrode (model 9617B). <sup>1</sup>H-NMR spectra were recorded at 400 MHz with a quad probe using CDCl<sub>3</sub> as the solvent and *p*-xylene as the internal reference. A MARS<sup>TM</sup> multimode microwave reactor (CEM Corp.) was used for polymerizations. UV/Vis spectra were recorded on a Hewlett Packard 8452A diode array spectrophotometer using HP 8953K UV/Vis kinetics software.

**Particle Size Characterization.** Particle size distributions were determined by Scanning Electron Microscopy (SEM, JSM-6360, JEOL), dynamic light scattering (DLS, Malvern HPPS 3.1 instrument equipped with He-Ne, 3.0 mW, 633 nm a laser) and by optical microscopy (DMIRB, LEICA Microsystems). A copolymer dispersion of 5-6 drops was diluted to 10 mL with HFE-7200 and filtered through cotton for DLS measurements. After the sample stood at 25 °C in the cell chamber, the particle size and size distribution were determined. SEM samples were prepared by placing two drops of diluted dispersion onto freshly cleaved mica sheet (1 cm)<sup>2</sup> mounted on an aluminum stub, dried at room temperature and coated with 10-15 nm of gold. The SEM accelerating voltage applied was 5 kV. Powdered quaternized polymers (**6**, **7**, and **8**) were spread on a

microscope slide to measure the particle size by optical microscopy. Mean diameters of 50 particles were calculated from SEM and optical micrographs.

**Copolymerization of 2-EHMA and OFPM.** EHMA (0.61 mmol, 0.14 mL), OFPM (0.39 mmol, 0.08 mL), *p*-xylene (0.5 mmol, 0.06 mL), AIBN (0.125 mmol, 0.020 g), and CDCl<sub>3</sub> (0.32 mL) were mixed, and transferred to an NMR tube under N<sub>2</sub>. Copolymerization was carried in an NMR tube at 50 °C for 10 h, and the <sup>1</sup>H-NMR spectra were obtained every 2 h for 10 h. In the first two hours copolymer conversion reached 20 %. Amounts of monomers remaining were calculated from the areas of their signals at 5-6 ppm relative to the area of *p*-xylene signal at 7.1 ppm. After 10 h 11 % of EHMA and 8 % of OFPM remained.

**Conventional Dispersion Polymerization.**<sup>7,37-39</sup> All the dispersion polymerizations were carried out in an inert fluorinated solvent HFE-7200, and the monomer content was kept at 10 wt %. All 2-EHMA conventional dispersion polymerizations with or without semifluorinated vinyl monomers were performed in 1 % HDF treated flasks. A 250 mL, round bottom flask, was filled with 1 % HDF in toluene and fitted with a glass stopper was heated in an oil bath at 100 °C for 1-2 days. The flask was rinsed with HFE-7200 before use for conventional polymerizations. Microwave polymerizations were performed under pressure in closed vessels. All glassware was oven-dried and purged with nitrogen.

A 250-mL, a three-necked round bottom flask fitted with a rubber septum, a reflux condenser equipped with nitrogen inlet, and a mechanical stirrer fitted with Teflon blade was filled with nitrogen at room temperature. Care was taken to ensure that the stirrer was always at the same distance (5 mm) from the bottom of the reactor during the

polymerization. The stirring rate was controlled at 300 rpm. HFE-7200 (149 mL) was charged to the flask and flushed with nitrogen for 15 min under continuous stirring. To this flask, nitrogen purged 2-EHMA (12.6 g), VBC (4.18 g), and DVB (0.17 g) were added and stirred at room temperature. After 30 min, the flask containing homogenous solution was placed in an oil bath at 60 °C under slight positive pressure of nitrogen. AIBN (0.167 g) dissolved in 1 mL of HFE-7200 was charged to the flask. After 50-55 min, the mixture turned milky due to nucleation of the particles. The mixture was kept at 60 °C for 24 h after nucleation. These dispersions were stable for 1-3 h during polymerization before foam appeared. Separation of foam from the liquid by vacuum filtration and drying gave solid polymer (**1**). EHMA copolymer dispersions were collected at 20 min intervals from the nucleation to the foamy stage to monitor the progress of the polymerization using <sup>1</sup>H-NMR and DLS.

The same procedure was also used for copolymerization of 2-EHMA with OFPM and PFDM. Copolymerization of 72 wt % EHMA, 25 % VBC, and 1 % DVB with 2 % OFPM to give polymer **2**, and with 2 % PFDM, gave polymer **3**. All of the conventional copolymerizations in nonafluorobutyl ethyl ether without (**1**) or with 2 wt % of OFPM (**2**) or PFDM (**3**) and with 10 wt % PPFOA (**4**) gave foamy mixtures. The products were obtained by vacuum filtration of the foam and by scraping solid from the inner walls of the flask. The combined solids were dried under vacuum and stored in an oven dried amber color vial for further experiments. Dried solid (10 mg) of EHMA copolymer with OFPM (**2**) was analyzed for carbon, hydrogen, and fluorine content. Anal. calcd for (C<sub>12</sub>H<sub>22</sub>)<sub>0.72</sub> (C<sub>7</sub>H<sub>7</sub>)<sub>0.25</sub> (C<sub>7</sub>H<sub>7</sub>F<sub>8</sub>)<sub>0.02</sub> (C<sub>10</sub>H<sub>10</sub>)<sub>0.01</sub>: C, 76.02; H, 10.15; F, 5.06. Found: C, 68.22; H, 8.28; F, 5.1.



**Bulk Polymerization of PFOA.** Synthesis of poly(perfluorooctyl acrylate) was reported in the literature.<sup>28</sup> 1H,1H-Perfluorooctyl acrylate (PFOA, 5.0 g,  $1.1 \times 10^{-2}$  mol) was added to a nitrogen filled 25-mL, two-necked, round bottom flask fitted with a rubber septum, a reflux condenser equipped with nitrogen inlet, and magnetic stirrer. PFOA was stirred for 30 min under nitrogen at room temperature. At 65 °C, AIBN (0.025 g,  $1.5 \times 10^{-4}$  mol) was added and the mixture was stirred for 20 h. Crude product was dissolved in a mixture of PFP and CH<sub>2</sub>Cl<sub>2</sub> and precipitated into methanol. Poly(perfluorooctyl acrylate) (PPFOA) was vacuum filtered and dried for 48 h. The synthesis of the PPFOA (**4**) is in Scheme 3.

**Microwave Dispersion Polymerization in HFE-7200.** A 50-mL, two-necked, round bottom flask equipped with a Teflon-coated magnetic stirbar, rubber septa, and a stopcock inlet was filled with nitrogen. HFE-7200 (17.9 mL) was charged to the flask and flushed with nitrogen for 15 min under continuous stirring. To this flask, nitrogen purged 2-EHMA (74 wt %, 1.48 g), VBC (25 wt %, 0.50 g), and DVB (1 wt %, 0.02 g) were added in a sequential manner and stirred for 30 min. PPFOA (10 wt %, 0.2 g) and AIBN (1 wt %, 0.02 g) were added at 10 min intervals and the contents were stirred for 30 min. The contents of the flask were transferred to a 20 mL glass tube of the MARS<sup>TM</sup>. The microwave reactor was programmed (P = 200 psi, T = 70 °C, power = 70 % of 400 W) for 4-5 h polymerization with medium stirring speed. The cross-linked copolymer of EHMA, VBC, DVB, and PPFOA (**5**) was obtained as a stable dispersion.

**Solid Content of Latexes.** The solid content of the stable latexes was determined by accurately weighing 1 mL of the latex and drying to constant weight in a water bath at

50 °C. Determinations performed in triplicate were reproducible to within 3 % of the mean.

**Conventional Quaternization of Solid Polymers 1, 2, and 3.** A mixture of 2-EHMA cross-linked copolymer **1** (1.5 g, 2.4 mmol of VBC groups), 20-30 mL of HFE-7200 and anhydrous trimethylamine (3.8 g, 64.5 mmol) was transferred to a stainless steel reactor and sealed. This mixture was stirred magnetically for 48 h at 60 °C. The excess trimethylamine was evaporated in a fume hood by bubbling argon through polymer particles for 4 h. Further, the solid polymer (**6**) was dried under argon for 2-3 days. Similar quaternizations were carried out on the polymers **2** (2-EHMA-OFPM) and **3** (2-EHMA-PFDM) with anhydrous trimethylamine. Solid polymers were freeze-dried and ground to a fine powder. The light yellow color solids were stored in an amber color vial in the dark at room temperature for further experiments.

**Microwave Quaternization of Stable Polymer Particles 5.** Stable cross-linked copolymer (**5**) dispersion in HFE-7200 (5 mL) containing 0.25 g of polymer was diluted with 20 mL of HFE-7200. This diluted dispersion and 0.64 g of anhydrous trimethylamine (10.7 mmol) were transferred to a 20 mL glass tube of the MARS™ reactor and sealed. Microwave reactor was programmed (P = 200 psi, T = 60 °C, power = 70 % of 400 W) for 1 h 15 min. The excess trimethylamine was evaporated by bubbling argon through the mixture (2-EHMA-PPFOA-TMA, (**9**)) for 4 h in a fume hood. The light yellow color stable polymer was stored in a scintillation vial at 5 °C.

**Determination of Chloride Content for Quaternized Solid (6, 7, and 8) and Stable Colloidal Polymers (9).** Quaternary ammonium chloride contents of the latexes were measured by potentiometric titration with a chloride selective electrode. To a 50 mL

beaker was added 50 mg of the powdered latex, 0.6 mL of 5 M NaNO<sub>3</sub>, and 20-25 mL of water to cover the tip of the electrode. The pH of the solution was adjusted to 2 with 1 M HNO<sub>3</sub> and the mixture was titrated with standard 0.05 M AgNO<sub>3</sub>. A titration curve of millivolts vs. milliliters of titrant was constructed, and the end point was taken as the point of maximum slope.

For stable dispersions, an accurately measured 1 mL of EHMA cross-linked copolymer was added to a 50 mL beaker and dried under nitrogen. To this was added 1 mL of THF to swell the polymer, 0.5 mL of 5 M NaNO<sub>3</sub>, and 20-25 mL of water to cover the tip of the electrode. The rest of the procedure was same for the solid polymers.

**Hydrolysis of PNP<sub>H</sub> by Coagulated Polymer Particles (6, 7, and 8) in NaOH Solution.** A stock solution of *p*-nitrophenyl hexanoate (PNPH, 2.5 mM) for kinetic measurements was prepared in acetonitrile on the day of use. The NaOH solution of 0.01M was prepared using nitrogen-purged water and was stored in an air-tight container. Molar extinction coefficient ( $\epsilon$ ) and  $\lambda_{\text{max}}$  for PNP<sub>H</sub> were calculated by measuring the absorbance of 2.5 mM PNP<sub>H</sub>/CH<sub>3</sub>CN in HFE-7200 and the values were 5488 L mol<sup>-1</sup>cm<sup>-1</sup> and 290 nm. The  $\epsilon$  and  $\lambda_{\text{max}}$  for PNPO<sup>-</sup> were determined after heating a solution containing 0.1 mL of 2.5 mM PNPA/ CH<sub>3</sub>CN and 2.9 mL of 0.1 M NaOH in scintillation vial at 50 °C. PNPO<sup>-</sup> absorbance reached maximum and attained constant in 72 h. The  $\epsilon$  and the  $\lambda_{\text{max}}$  values for PNPO<sup>-</sup> were 21,440 L mol<sup>-1</sup>cm<sup>-1</sup> and 400 nm. The following kinetic run is typical. A 1-cm quartz cuvette was filled with 3.0 mL of 0.01M NaOH solution, and the cuvette was stoppered and placed in the sample chamber of a Cary 5000 UV-VIS spectrophotometer thermostated at 30.0 ± 0.1 °C. After 20 min of stirring, 1.0 mg of solid copolymer (6) wetted with 1-2 drops of acetonitrile was added and mixed by

rapidly shaking the cuvette for 2 s. PNPB solution (5  $\mu$ L, 2.5 mM) was added, and a UV-VIS spectrum was taken every min for 10 min. The Abs at 400 nm was plotted as a function of time. The same experiment was repeated under identical conditions but using 5  $\mu$ L of 2.5 mM stock solution of *p*-nitrophenyl hexanoate (PNPB) in isopropyl alcohol in 2 mL HFE-7200.

**Hydrolysis of PNPB by Coagulated Polymer Particles (6, 7, and 8) in HFE-7200.** The physical mixing of two different phases during the hydrolysis was improved by shaking the mixture with a mechanical shaker. The dried solid polymer (6, 10.0 mg, 16  $\mu$ mol of N<sup>+</sup>) and 3 mL of HFE-7200 were placed in a polystyrene cuvette. This suspension containing the particles and HFE-7200 was equilibrated by shaking for 20 min to at 150 rpm. PNPB in acetonitrile (20  $\mu$ L, 2.5 mM) was added and continued shaking for 2-20 min. The supernatant was collected to record the absorbance of PNPB. The UV-Vis spectrum of the supernatant had no peak at 290 nm corresponding to PNPB indicating that PNPB was completely absorbed by the particles. PNPB absorbed polymer particles were mixed with 0.5 mL of NaNO<sub>3</sub> (1 M, pH 9) by shaking for 2 min at 150 rpm to displace PNPO<sup>-</sup> by NO<sub>3</sub><sup>-</sup>. This displacement step was repeated three times, and each time the aqueous phase was collected and diluted to 3 mL with DI water to monitor the conversion of PNPB to *p*-nitrophenoxide (PNPO<sup>-</sup>) ion at 400-410 nm.

**Ion-Exchange of Coagulated Polymer Particles (6, 7, and 8) Loaded with Cl<sup>-</sup> by OH<sup>-</sup>.** In this method, 10 mg (16  $\mu$ mol of N<sup>+</sup>) of solid copolymer (6), and 10 mL of THF were taken in a scintillation vial and were evacuated for 60 min to remove the air trapped in the particles and to wet the particles. The solvent was removed by a pipette, and the wet particles were treated with excess (5 mL of 0.01 M, 50  $\mu$ mol) NaOH to

replace the  $\text{Cl}^-$  of polymer particles with  $\text{OH}^-$ . The supernatant was decanted and the polymer particles were washed 4-5 times with DI water to remove excess  $\text{OH}^-$  and  $\text{NaCl}$  until the pH of the supernatant was 7. Finally, the particles containing  $\text{OH}^-$  and 5 mL of (1 M, pH 9)  $\text{NaNO}_3$  were mixed by shaking to displace  $\text{OH}^-$  by  $\text{NO}_3^-$ . This displacement step was repeated two times. The collected supernatant was titrated against standard 0.01 M  $\text{HCl}$  using phenolphthalein indicator. Same procedure was used for copolymers **7** and **8**.

The solid polymer (**6**, 0.50 g) and 10 mL of THF were added to a scintillation vial. This dispersion was evacuated for 60 min to remove air trapped in the particles and to swell the polymer particles. The THF was decanted, and the polymer particles were re-dispersed in 15 mL of  $\text{NaOH}$  (1 M) and mixed by shaking for 40 min at 150 rpm for ion-exchange of  $\text{Cl}^-$  by  $\text{OH}^-$ . The supernatant was decanted and the particles were redispersed in DI water and continued shaking for 20 min to remove the excess of  $\text{OH}^-$ . This cycle was repeated four times until the supernatant pH is 7. The particles in  $\text{OH}^-$  form were vacuum filtered and stored in an amber color vial for further use. Similar procedure was used for the ion-exchange of solid polymers **7** and **8**.

**Hydrolysis of PNPH by Wet Coagulated Polymer Particles (6, 7, and 8).** A 40 mg sample ( $64 \times 10^{-3}$  mmol of  $\text{N}^+$ ) of wet polymer (**6**) was placed into a polystyrene cuvette and 3 mL of HFE-7200 was added. This dispersion was mixed by shaking to equilibrate the particles and HFE-7200 for 20 min at 150 rpm. PNPH in isopropyl alcohol (20  $\mu\text{L}$ , 2.5 mM) was added and continued shaking for 2-20 min. The supernatant was decanted. The polymer particles and 0.5 mL of  $\text{NaNO}_3$  (1 M, pH 9) were mixed by shaking for 2 min at 150 rpm to displace  $\text{PNPO}^-$  by  $\text{NO}_3^-$ . This step was repeated three times, and each time the aqueous phase was collected and diluted to 3 mL with DI water

to monitor the conversion of PNP<sub>H</sub> to PNPO<sup>-</sup> ion at 400-410 nm by UV-Vis spectrophotometer.

**Hydrolysis of PNP<sub>H</sub> by Stable Polymer Particles (9) Loaded with Cl<sup>-</sup> Ion in HFE-7200 and Borate Buffer Mixture.** A stock solution of *p*-nitrophenyl hexanoate (PNP<sub>H</sub>, 2.5 mM) in acetonitrile was prepared on the day of use. Borate buffer (0.02 M) solution was prepared from boric acid/water aqueous solution and the pH was adjusted to 9.38 using solid NaOH. To a 50-mL, round bottom flask, 50-100 μL (2-4 mg, 2.3x10<sup>-6</sup>-4.6x10<sup>-6</sup> mmol of N<sup>+</sup>) of polymer particles in HFE-7200, 1.0 mL of HFE-7200, and 9.0 mL of borate buffer were added in a sequence and stirred magnetically in an incubator for 30-60 min at 30 ± 1°C. PNP<sub>H</sub> in acetonitrile (368 μL, 2.5 mM) was added to the above mixture and stirring continued (30 ± 1°C). At the same time a quartz sub-microcell (path length (b) = 1 cm, V = 150-200 μL) was thermostated at 30.0 ± 0.1 °C in cell chamber. The supernatant of 100-150 μL was transferred to 1 cm path length cell to record the UV-Vis spectra of PNPO<sup>-</sup> every 2 min for 60 min.

The value of  $k_{\text{obs}}$  was calculated by the kinetics application in the manner of  $\ln [(A_{\infty}-A_0)/(A_{\infty}-A_t)]$  vs time. The values of  $A_{\infty}$  were determined manually and calculations were made from data over a time corresponding to 80% conversion. The data fit pseudo first-order kinetics. Rate constants measured in duplicate differed by 5- 10 %.

## References

1. Yang, Y.; Baker, J. A.; Ward, J. R. *Chem. Rev.* **1992**, *92*, 1729-1743.
2. Wagner, G. W.; Yang, Y. -C. *U. S. Patent* 6,245,957, **2001**, 1-10.
3. Talmage, S. S.; Watson, A. P.; Hauschild, V.; Munro, N. B.; King, J. *Current. Org. Chem.* **2007**, *11*, 285-298.
4. Yang, Y. -C. *Acc. Chem. Res.* **1999**, *32*, 109-115.
5. Wagner, G. W.; Yang, Y. -C. *Ind. Eng. Chem. Res.* **2002**, *41*, 1925-1928.
6. Kendall, J. L.; Canelas, D. A.; Young, J. L.; DeSimone, J. M. *Chem. Rev.* **1999**, *99*, 543-563.
7. Miller, P. D.; Ford, W. T. *Langumir* **2000**, *16*, 592-596.
8. Gedye, R.; Smith, F.; Westaway, K.; Ali, H.; Baldisera, L.; Laberge, L.; Rousell, J. *Tetrahedron Lett.* **1986**, *27*, 279-282.
9. Giguere, R. J.; Bray, T. L.; Duncan, S. M.; Majetich, G. *Tetrahedron Lett.* **1986**, *27*, 4945-4958.
10. Bogdal, D.; Penczek, P.; Pielichowski, J.; Prociak, A. *Adv. Polym. Sci.* **2003**, *163*, 193-263.
11. Wiesbrock, F.; Hoogenboom, R.; Schubert, U. S. *Macromol. Rapid. Commun.* **2004**, *25*, 739-1764.
12. Hoogenboom, R.; Schubert, U. S. *Macromol. Rapid. Commun.* **2007**, *28*, 368-386.
13. Sinnwell, S.; Ritter, H. *Aust. J. Chem.* **2007**, *60*, 729-743.
14. Loupy, A. Ed., *Microwaves in Organic Synthesis*; Wiley-VCH: Weinheim, **2006**, pp 327-361.

15. Chia, L. H.; Jacob, J.; Boey, C. Y. F. *J. Polym. Sci., Part A: Polym. Chem.* **1996**, *34*, 2087-2094.
16. Palacios, J.; Sierra, J.; Rodriguez, P. M. *New Polym. Mater.* **1992**, *3*, 273.
17. Jovanovic, J.; Adnadjevic, B. *J. Appl. Polym. Sci.* **2007**, *104*, 1775-1782.
18. Brown, S. L.; Rayner, C. M.; Perrier, S. *Macromol. Rapid. Commun.* **2007**, *28*, 478 - 483.
19. Zhu, X.; Zhou, N.; He, X.; Cheng, Z.; Lu, J. *J. Appl. Polym. Sci.* **2003**, *88*, 1787-1793.
20. Cheng, Z.; Zhu, X.; Chen, J.; Lu, J. *J. Macromol Sci., Pure Appl. Chem.* **2003**, *A40*, 1157-1171.
21. Stange, H.; Greiner, A. *Macromol. Rapid. Commun.* **2007**, *28*, 504-508
22. Zhu, X.; Chen, J.; Zhou, N.; Cheng, Z.; Lu, J. *Eur. Polym. J.* **2003**, *39*, 1187-1193.
23. Zhu, X.; Chen, J.; Cheng, Z.; Lu, J.; Zhu, J. *J. Appl. Polym. Sci.* **2003**, *89*, 28-35.
24. Xu, Z.; Hu, X.; Li, X.; Yi, C. *J. Polym. Sci., Part A: Polym. Chem.* **2007**, *46*, 481-488.
25. Sierra, J.; Palacios, J.; Vivaldo-Lima, E. *J. Macromol. Sci., Part A: Pure Appl. Chem.* **2006**, *43*, 589-600.
26. Albert, P.; Hölderle, M.; Mülhaupt, R.; Janda, R. *Acta Polymer* **1996**, *47*, 74-78.
27. Zhang, C.; Liao, L.; Gong, S. *Green Chem.* **2007**, *9*, 303-314.
28. Shiho, H.; DeSimone, J. M. *Macromolecules* **2001**, *34*, 1198-1203.
29. Kendall, J. L.; Canelas, D. A.; Young, J. L.; DeSimone, J. M. *Chem. Rev.* **1999**, *99*, 543-563.
30. Bodgal, D.; Pielichowski, J. P.; Prociak, A. *Adv. Polym. Sci.* **2003**, *163*, 193-263.



31. Wiesbrock, F.; Hoogenboom, R.; Schubert, S. U. *Macromol. Rapid. Commun.* **2004**, *25*, 1739-1764.
32. Herrero, M. A.; Kremsner, J. M.; Kappe, C. O. *J. Org. Chem.* **2008**, *73*, 36-47.
33. Leadbeater, N. E.; Torenius, H. M. *Microwaves in Organic Synthesis*; Loupy, A., Ed.; Wiley-VCH: Weinheim, 2006, p 327-361.
34. Tomoi, M.; Ford, W. T. *J. Am. Chem. Soc.* **1980**, *102*, 7140-7141.
35. Tomoi, M.; Ford, W. T. *J. Am. Chem. Soc.* **1981**, *103*, 3821-3828.
36. Tomoi, M.; Ford, W. T. *J. Am. Chem. Soc.* **1981**, *103*, 3828-3832.
37. Ford, W. T.; Liu, G. *Langumir* **2000**, *16*, 8814-8819.
38. Lee, J. -J.; Ford, W. T. *J. Am. Chem. Soc.* **1994**, *116*, 3753-3759.
39. Miller, P. D.; Spivey, H. O.; Copeland, S. L.; Sanders, R.; Woodruff, A.; Gearhart, D.; Ford, W. T. *Langumir* **2000**, *16*, 108-114.

## **CHAPTER III**

### **SYNTHESIS OF POLY (METHYL METHACRYLATE) CORE-SHELL LATEXES FOR COLLOIDAL CRYSTALLINE FILTER**

#### **Introduction**

Monodisperse polymeric colloidal spheres with diameters in the range of 10 nm to 1  $\mu\text{m}$  are of great interest. The controlled size and surface properties enable them to self-assemble into colloidal crystalline arrays with well-defined structures. Novel light diffraction and photonic bandgap properties of colloidal crystals are promising for fabrication of filters and sensors. Various methods to prepare polymeric colloidal spheres are dispersion polymerization, and emulsion polymerization. Dispersion polymerization was developed to synthesize monodisperse particles but uses polar organic solvents, which may cause environmental concern. Emulsion polymerization with/without emulsifier can produce uniform size latex particles in a size range of <50 nm to 2.5  $\mu\text{m}$ .<sup>1-7</sup> Emulsion polymerization in an aqueous medium is an important process for the production of polymer latexes containing reactive functional groups such as hydroxyl, aldehyde, carboxylic acid, amino, epoxy, sulfhydryl, succinimide, benzotriazole and chloromethyl groups.<sup>8</sup> The dispersions are stabilized by electrostatic repulsions among

the particles of the same sign of charge or steric factors arising from unfavorable entropy of mixing polymer chains that are bound to the particle surface. The early formation and the growth of the electrostatically stabilized particles prevent the formation of new particles, which lead to monodisperse latexes.

Monodisperse spheres of emulsion polymers form colloidal crystalline films (CCF) that are opalescent due to diffraction of visible light. Annealing transforms porous CCF's to thin films of interconnected colloidal arrays with interstitial spaces. These narrowly distributed pores will serve as separation channels. Aqueous emulsion polymerization produces uniform size particles and also allows controlling particle size and surface modification during the synthesis. These controlled size particles will be used to pack size-selective membranes.<sup>9</sup>

The objective of this research is to make sub-micron sized PMMA core-shell latex and to use the particles to construct latex composite membranes (LCM) for separation purposes. LCMs are formed by placing a polymer latex dispersion of monodisperse particles on to the surface of porous nylon support. Further, latexes are transferred to colloidal crystalline films by use of slow settling of the particles or fluidic cell approach. These particles form hexagonally and more uniformly packed thin array (film) with interstitial spaces serving as pores for size discrimination. Nylon support provides mechanical stability for the membrane. The membrane is stabilized by chemical or physical linking of contacts between the particles, usually reaction of carboxylic acid with glycidyl methacrylate repeat units in the shell of latex or by the inter diffusion and entanglement of polymer chains between the particles. LCMs will be characterized by microscopy techniques (scanning electron microscopy (SEM), atomic force microscopy

(AFM)). Finally, the selectivity and the efficiency of these more uniformly packed membranes will be compared to that of randomly packed and commercial membranes of comparable pore sizes using a mixture of dextrans of different sizes.

For this purpose, monodisperse PMMA core-shell latexes were synthesized using emulsifier-free aqueous emulsion polymerization and potassium persulfate as an initiator at 80 °C. Batch and seeded emulsion polymerizations were carried at 80 °C to develop the PMMA core. Starved emulsion polymerization was adopted to place the shell on these core particles. The PMMA core was coated with a mixture of methyl methacrylate (monomer), acrylic acid (functional monomer), butyl acrylate (softens the shell), glycidyl methacrylate, and allyl methacrylate as cross-linking agents. The latex polymer has glass transition temperature high enough to prevent coalescence during processing, and a shell that is soft to avoid fragility of a glass, and to cross-link particles in contact in the colloidal crystal. LCM's were made by flow cell method and a gravitational sedimentation-solvent evaporation method.

## **Results**

The goal of this research was to develop size selective latex composite membranes using monodisperse sub-micron PMMA core-shell latex particles for separation of nanometric particles and solutes in the water and compare the efficiency of LCM's with 80-90 nm pore size to that of randomly packed latexes and commercial membranes of comparable pore sizes using mixture of dextrans and various monodisperse polystyrene latexes of diameters in the range of 50 nm-200 nm. Batch, seeded, and starved semi-continuous emulsion polymerizations were used to synthesize

sub-micron monodisperse PMMA core-shell polymer particles with a 500 nm diameter core and a 28 nm annular thick shell. The overall syntheses are outlined in Schemes 1-3. All the polymerizations were performed in water. All the three methods reported here, batch, seed growth, and starved-emulsion polymerizations, were reproduced at least three times during this research.

Among all the three methods, PMMA core preparation by batch polymerization and shell growth by starved semi-continuous methods are easy and simple whereas seed growth core by a seeded emulsion process is tricky and time consuming. It took much time to synthesize a stable, monodisperse, submicron seed growth core by seeded emulsion polymerization. The most common problem with this method is the secondary particle generation. All attempts to synthesize stable seed growth core using various reaction conditions such as equilibration time, increased amount of initiator, and reduced amount of monomer and no extra water gave bimodal latexes except the procedure reported here.

**Batch Polymerization (1).** In batch polymerization water insoluble methyl methacrylate was stirred with water to form monomer droplets and a small quantity of dissolved monomer as shown in Scheme 1. This heterogeneous dispersion was heated to 80 °C and potassium persulfate initiator was added. This charged initiator provides the stabilizing groups on the particle surface. Thermal decomposition of the initiator started polymerization of the small amount of methyl methacrylate in the aqueous phase. Oligomeric poly(methyl methacrylate) chains began to form in the aqueous phase until they reach a size that was too large to be soluble. These chains then aggregated to form primary particles which continued to grow by monomer swelling by the diffusion of

monomer from droplets through water and into the particles the aqueous phase. This process was continued until all the methyl methacrylate was consumed to form the stable particles. This method produced stable emulsion of PMMA core particles (sample 1, Table 1), as shown in the AFM image of Figure 1.

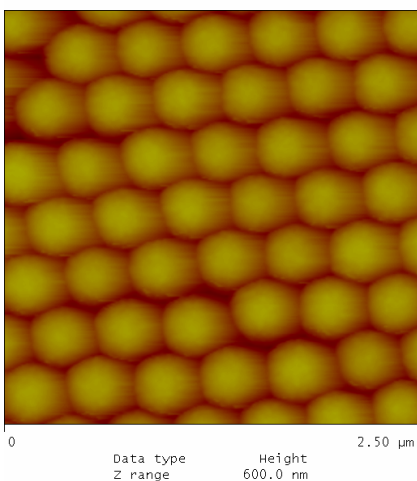
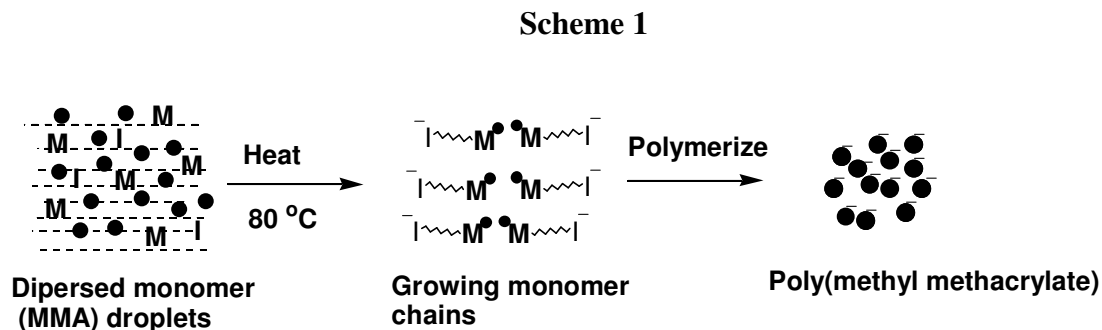
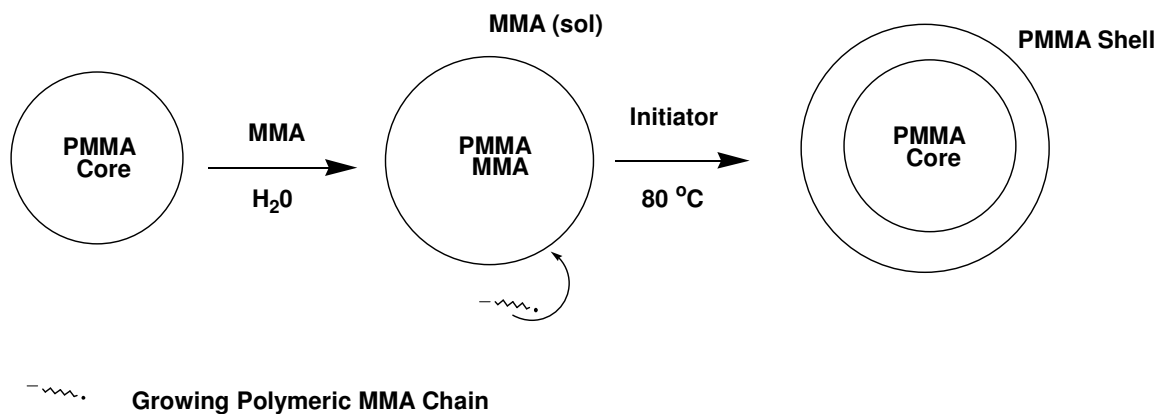


**Figure 1.** AFM image of the 400 nm PMMA core latex (1) on a mica surface.

**Seeded Emulsion Polymerization (2).** Sub-micron PMMA seeded core was made by seeded emulsion polymerization (Scheme 2) in which preformed PMMA seed latex of 400 nm was swollen with methyl methacrylate for 24 h. After swelling was

complete, thermal decomposition of the initiator initiated the polymerization preferably from the solution to form the polymeric chains. The growing polymeric chains were collided with monomer swollen latex to begin polymerizing the monomer inside. This resulted in stable emulsion of monodisperse seeded PMMA core latex (sample 2, Table 1), as shown in the AFM and SEM images (Figures 2, 3).

**Scheme 2**



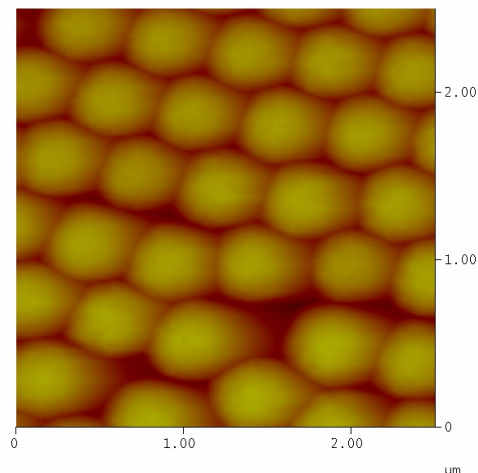


**Figure 2.** AFM image of the 500 nm PMMA seed growth latex (2) on a mica surface.

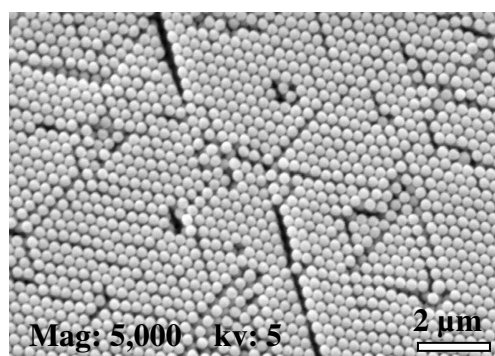


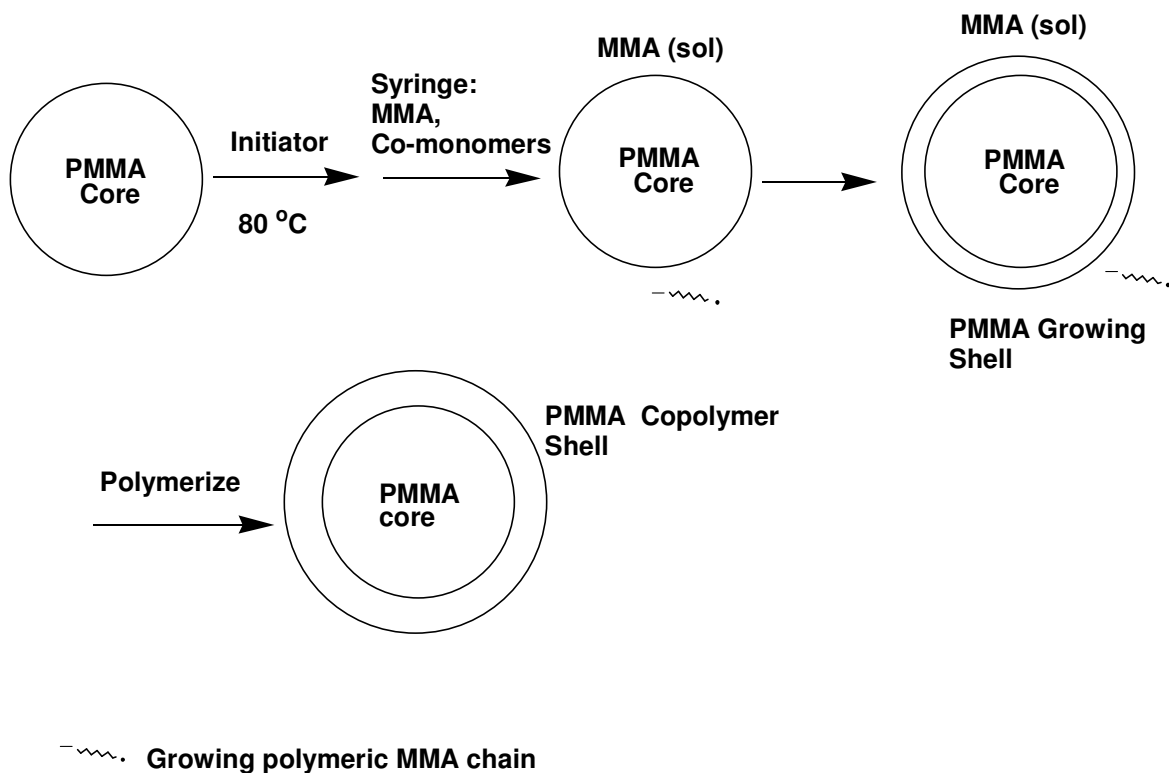
**Figure 3.** SEM image of the 500 nm PMMA seeded core latex (2) on a silica surface.

**Shell Growth by Starved Semi-Continuous Polymerization (3).** In this polymerization, a mixture of monomers of methyl methacrylate (59 %), (4.0 %) of allyl methacrylate, (3.8 %) of acrylic acid, (15.6 %) of glycidyl methacrylate and (17.7 %) of butyl acrylate was added slowly to the reaction vessel that contained PMMA seeded core latex (17.2 g) and initiator. Since most of the second stage monomeric mixture was in the aqueous phase and only residual monomers were in the seed latex, polymerization was



initiated in the aqueous phase to form oligomeric chains. Shell formation was the result of monomer polymerizing near the surface of the particle which was faster than diffusion of growing polymer chains into the core of the particle. The growing polymer chains collide with high surface area seed latex particles to form final latex particles. The amount of swelling was kept low due to continual entrance of growing radical chains and the slow rate of monomer addition. The overall growth of PMMA core-shell latex was kinetically controlled due to slow diffusion of polymer. This method gave a stable emulsion containing monodisperse core-shell latex particles (sample 3, Table 1) as shown in the AFM and SEM images (Figures 4, 5). The synthesis is outlined in Scheme 3.

**Scheme 3**



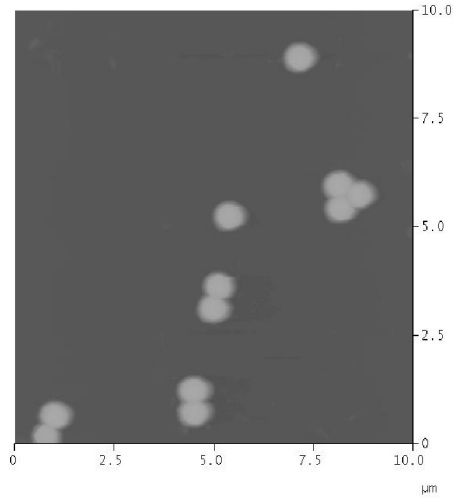


**Figure 4.** AFM image of the 555 nm PMMA core-shell latex (3) on a mica surface

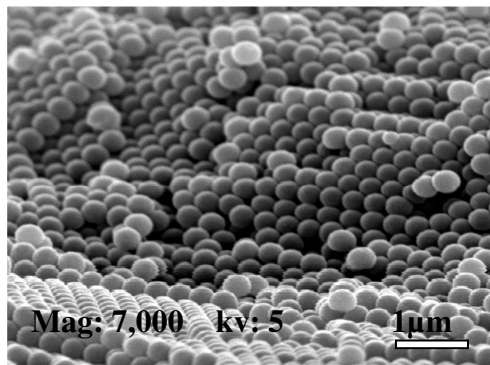


**Figure 5.** SEM image of the 555 nm PMMA core-shell latex (3) on a silica surface.

Monodisperse sub-micron PMMA core-shell latexes of diameter ratio 10 core: shell 1 were analyzed for particle size distributions by dynamic light scattering (DLS), AFM, and SEM. Dynamic light scattering studies revealed that the seeded core and core-shell

latex particles were 500 nm and 550 nm in size as shown in Table 1. Mean diameters and standard deviations of 50 particles were calculated using DLS and SEM data.

**Table 1. Particle Diameters for PMMA Core, Seeded Core and Core-shell Latexes**

Sample	Latex	Diameter (nm)		Polydispersity
		DLS	SEM <sup>a</sup>	Index <sup>b</sup>
1	PMMA Core	400	--	0.002
2	Seeded Core	460	500	0.006
3	Core-shell	554	555	0.01

<sup>a</sup>Standard deviation from measurement of diameters of 50 particles were less than 1 nm.

<sup>b</sup>DLS

To determine if a true core-shell latex was achieved, the diluted latex particle dispersions were deposited on freshly cleaved mica and silica surfaces at room temperature for particle size determination by AFM, and SEM. AFM images of core (Figure 1), and seeded core (Figure 2) indicated the increase in size of 400 nm to 500 nm whereas Figure 4 evidenced the presence of 55 nm copolymer shell on the PMMA sub-micron core. SEM studies on particle size distributions also proved that the increase in particles size from seeded core (500 nm) to core-shell latex have 555 nm as shown in Figures 3 and 5. We measured the diameter of the particle by measuring the distance between the centers of the adjacent particles. All three analyzes proved that PMMA core-shell latex particles are monodisperse and of 555 nm in size.

Uniform and sub-micron core-shell latex particles were used to prepare latex composite membranes (LCM's) for size selective filtration purposes. Size selectivity arises from the uniform size of interstices between uniform spheres packed into colloidal

crystalline layers (CC's). These CC's were transformed to interconnected arrays (LCM's) by annealing. LCM's can be formed either by physical annealing or chemical cross-linking. Physical stabilization will be based on interdiffusion and entanglement of polymer chains to make contacts between the particles.<sup>9</sup> Generally this will be achieved by partial annealing the latex particles at elevated temperatures. The glass transition temperature ( $T_g$ ) of the core and shell latex will define the conditions under which limited coalescence of the particles occurs without sufficient flow to fill in the pores.<sup>9</sup> Our differential scanning calorimetric studies on the sample (3) revealed that the  $T_g$  of our PMMA core was 124 °C and shell latex was 80 °C. We decided to stabilize our LCM's packed by partial annealing at 120 °C for an hour to form LCM. Chemical stabilization involves both interdiffusion of polymer chains as well as a chemical reaction at the point of contact between the particles.<sup>10-14</sup> For this reason we chose the shell consisting of functional monomers such as acrylic acid (AA) and glycidyl methacrylate (GMA). During the stabilization the reaction of epoxy group of GMA with carboxylic group of AA will occur to form the ester linkage.<sup>15-17</sup> Images of the top surfaces and cross-sections of these LCM's were obtained by SEM to determine structure and order of latex particles.

### **Colloidal Crystalline Filters**

Two different approaches were tried to pack these monodisperse PMMA core-shell latexes consisting of 500nm core and 55 nm shell.

**Gravitational Sedimentation and Solvent Evaporation.**<sup>9</sup> In this method, we tried to pack the diluted PMMA core-shell latex dispersion (3) to obtain a LCM of 130  $\mu\text{m}$  thickness. The basic principle involved in this was the particles settle to bottom of the

flask by gravity and simultaneous solvent evaporation made the particles packed into colloidal crystalline layers by capillary forces. The overall process was outlined in Figure 6. LCM's were packed on positively charged nylon support to improve the mechanical strength and were stabilized by annealing at 120 °C for one hour. Surface of the nylon support was rough with 0.2 μm pores. The support was washed with a cationic surfactant to place the anionic particles by electrostatic interaction. Annealing transformed the colloidal crystalline layers to interconnected colloidal crystalline arrays.

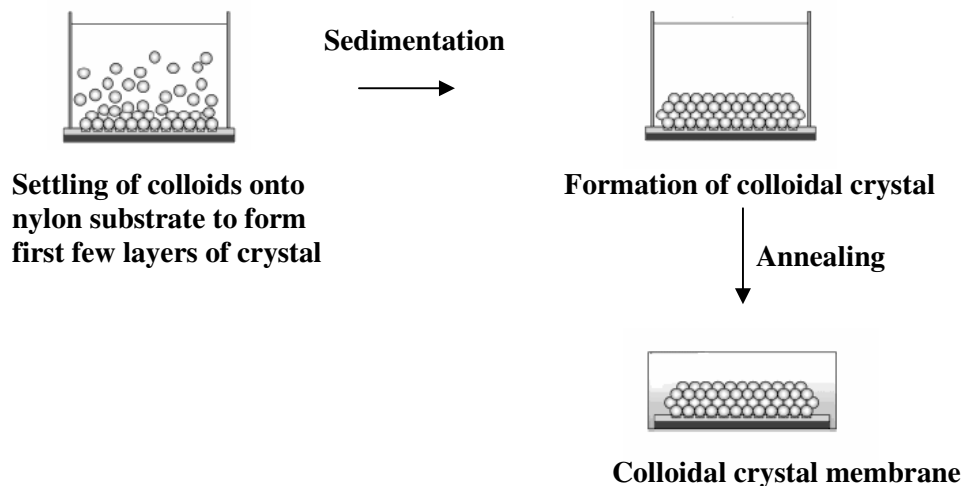


**Figure 6.** LCM's packing by gravitational sedimentation by solvent evaporation.

Permeability of the LCM's can be determined by filtering a commercially available mixture of dextrans and mixtures of different sizes of monodisperse polystyrene spheres. SEM images of these CC's before annealing and LCM's after annealing are shown in Figure 7 and the cross-sectional images of the fractured films are shown in Figure 8. SEM of the membranes showed small hexagonal domains of 5 μm size on the surface, with missing spheres, wide cracks, and disordered regions. Some of the pores in the cross-sectional images of the film are very much bigger than the pores between the

packed particles. All these defects in the film might limit the selectivity of the LCM for filtration purposes. These small colloidal crystalline lattices were obtained in 24-48 h. In order to minimize these defects; the CC's fabrication was repeated using Texanol with 12 h of evaporation time. Texanol (2,2,4-trimethyl-1,3-pentanediol monoisobutyrate) is a plasticizer which can decrease the  $T_g$  of the polymer and makes the shell soft. This will help particles to cross-link effectively during the stabilization. We developed the CC's using PMMA core-shell particles of 10 mL (0.6 wt % , 60 mg) of containing 10 wt % of Texanol (6 mg) with 12 h of evaporation time to obtain 28  $\mu\text{m}$  thickness. The surface of the CC film was not smooth enough and has very thick edges compared to the center. This film was transformed to LCM by annealing at 120  $^{\circ}\text{C}$ . SEM of the LCM has hexagonal domains of 5-10  $\mu\text{m}$  on the surface, with few missing spheres and wide cracks of 1-2  $\mu\text{m}$  as shown in Figure 9. Since gravitational sedimentation is very slow and time consuming we switched to sonication assisted packing to speed up the particle packing.

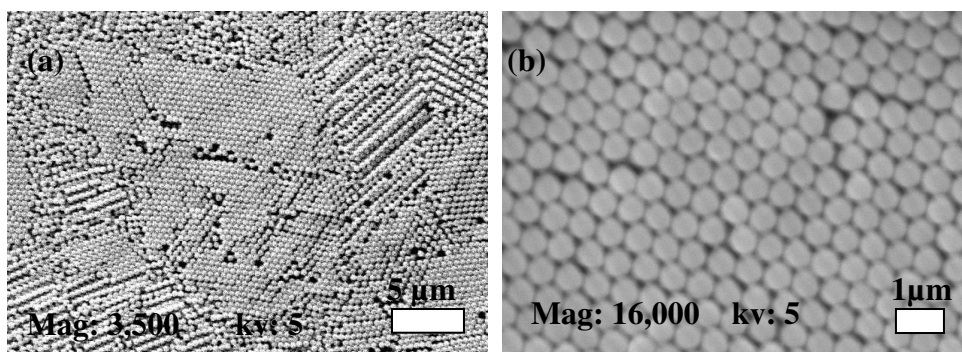


**Figure 7.** SEM image of the LCM made by gravitational sedimentation by solvent evaporation with no Texanol (sample 3, Table 1): (a) before annealing, (b) after annealing.

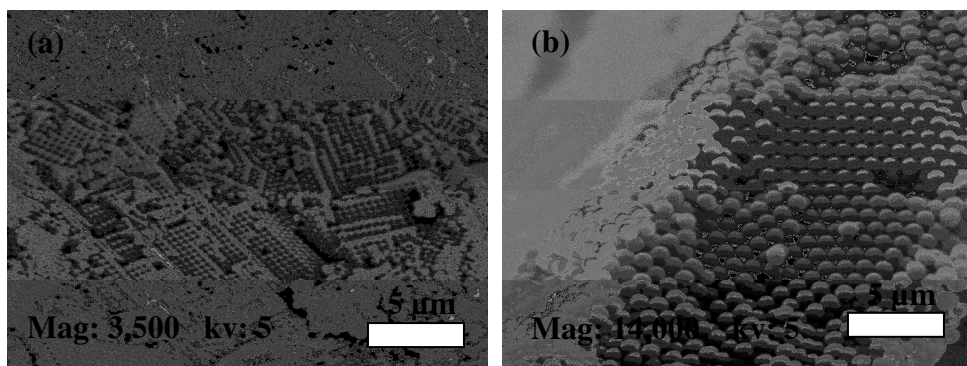


**Figure 8.** SEM image of the LCM: (a) center, (b) the edge (sample 3, Table 1).



**Figure 9.** SEM image of the LCM packed by gravitational sedimentation and solvent evaporation with 10 wt % Texanol (sample 3, Table 1).

**Fluidic Cell Approach by Sonication Assisted Packing.**<sup>18-21</sup> In this method, the diluted monodisperse PMMA core-shell latex dispersion was assembled in a packed cell of 2.5 (cm)<sup>2</sup> area to obtain the LCM's 130 μm thick. The type of cell used for making LCM's and the sonicator is shown in Figure 10. Thickness of the LCM film was controlled by thickness of the Mylar film between the two glass plates. In this method, the crystal nucleated from the bottom of the cell because the solvent could only leave the cell through the array of channels in the Mylar film. Mylar film was used as spacer to retain the latex particles as small as ~200 nm in size, and also its soft surface provides the

conformal contact between the two glass substrates and the polymer film. CC's were formed in 20-30 min. Once the crystal reached the required size, the packed cell was placed in an oven at 120 °C for 2-3 h to obtain interconnected colloidal crystalline array (LCM). The packed LCM was carefully detached from the packed cell to study the structure and order by SEM. The majority (Figure 11) of the surface of the LCM was amorphous with very small hexagonally packed domains, and wide cracks.

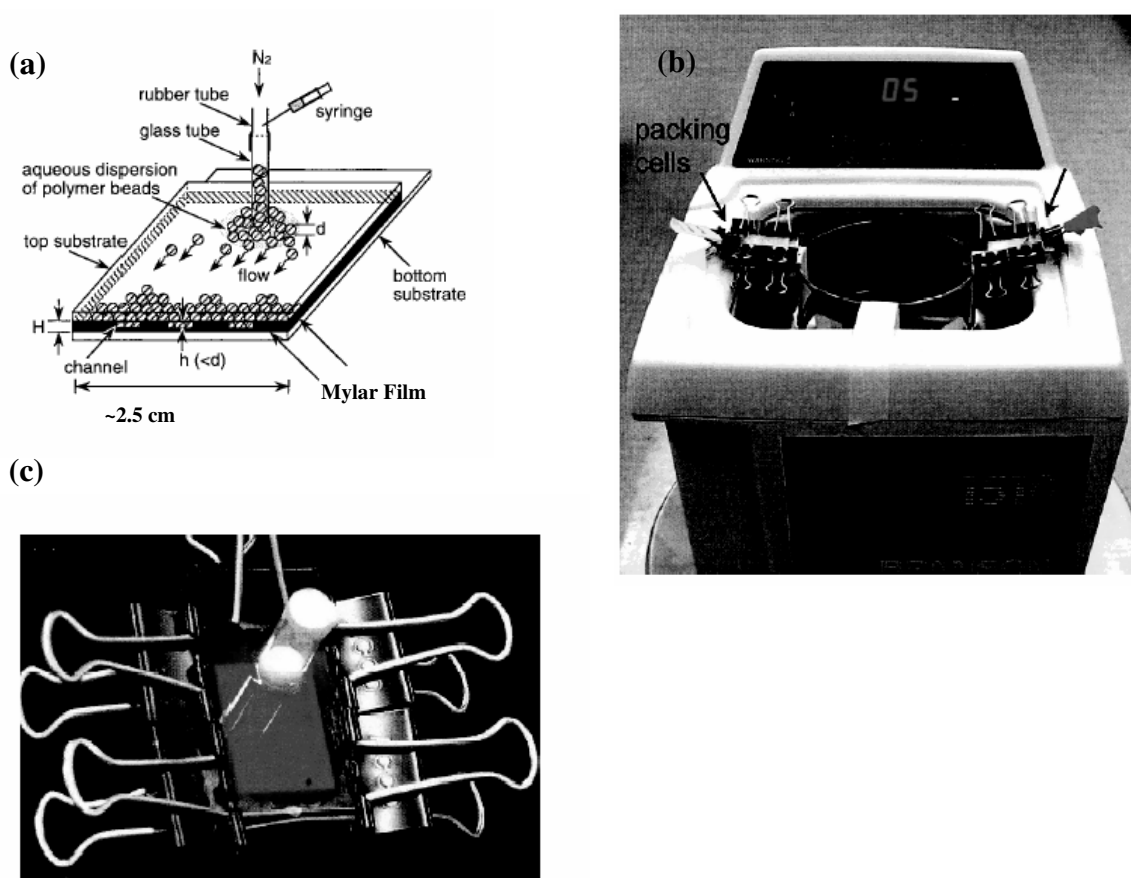


**Figure 10.** (a) Schematic diagram of fluidic cell. (b) Experimental setup showing the packing cells on the sonicator. (c) Packed cell constructed from Mylar film of 130  $\mu\text{m}$ . Ref 21.



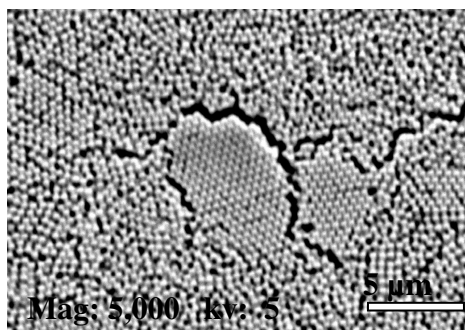


**Figure 11.** SEM image of the top surface of the LCM developed by sonication assisted method after annealing (sample **3**, Table 1).

## Discussion

Stable, monodisperse poly(methyl methacrylate) core-shell latexes of 10/1 diameter ratio were synthesized using batch, seeded, and starved semi-continuous polymerizations for making size selective colloidal crystalline membranes (LCM). PMMA core-shell latex was prepared using seed growth latex (**2**) as the core and the comonomers such as methyl methacrylate (monomer), acrylic acid (functional monomer), glycidyl methacrylate, butyl acrylate, and allyl methacrylate (cross-linking agent) to form the shell by starved semi-continuous polymerization. Butyl acrylate softens the shell by reducing the glass transition temperature ( $T_g$ ) of the polymer whereas acrylic acid and glycidyl methacrylate monomers provide the crosslink between the particles during the stabilization of the LCM. LCM's formed by gravitational sedimentation and solvent evaporation with 10 wt % plasticizer (Texanol) have hexagonally packed domains of 5-10  $\mu\text{m}$  on the surface with few point defects and cracks of 1-2  $\mu\text{m}$  compared to the regular sedimentation and sonication assisted packing methods. Since I was disappointed with top surface morphology of the LCM's I did not proceed for the filtration

experiments. Cell leaking was the major problem in packing the large cells of  $2.5 \text{ (cm)}^2$  area. LCM's formed by gravitational sedimentation by solvent evaporation using 10 wt % Texanol have hexagonally packed crystalline domains with fewer defects compared as shown in Figure 9 to LCM's formed by regular sedimentation (Figure 7) and sonication assisted packing (Figure 11). Since the particle synthesis by emulsion polymerization is very well known and easy, it is worth to repeat LCM packing by gravitational sedimentation method. Application of several layers of latex particles and stabilizing the array by gradual annealing to  $120 \text{ }^\circ\text{C}$  with  $10 \text{ }^\circ\text{C}$  raise in temperature might minimize the cracks and also cross-links the particles in the LCM. This might also serve the purpose of making 100-130  $\mu\text{m}$  thick films for the filtration purposes. Alternatively synthesis of core-shell latex particles with much softer shell would help to cross-link the particles during the stabilization to form uniform pores.

### **Summary**

Batch, seeded, emulsion polymerizations were used to synthesize monodisperse sub-micron PMMA core latexes. Starved emulsion polymerization was adopted to place the shell of 55 nm on these core particles. The PMMA core was coated with a mixture of methyl methacrylate (monomer), acrylic acid (functional monomer), glycidyl methacrylate, and allyl methacrylate as cross-linking agents and butyl acrylate to soften the shell. All these latex particles were characterized by DLS, AFM, and SEM analyses. The latex particles were spherical and  $0.55 \mu\text{m}$  in diameter. These uniform latex spheres make latex composite membranes (LCM) for the size selective filtration of nanometric

particles and solutes in the water. Gravitational sedimentation by solvent evaporation and fluidic cell approach by sonication assisted packing methods were used to pack the LCM of ~130  $\mu\text{m}$  thickness. LCM's obtained by gravitational sedimentation with 10 wt % Texanol showed hexagonally packed crystalline domains of 5-10  $\mu\text{m}$  size on the surface with the few missing spheres, and cracks of 1-2  $\mu\text{m}$  size whereas fluidic cell approach has more of amorphous domains than crystalline regions of 1-2  $\mu\text{m}$ .

## Experimental

**Materials.** Methyl methacrylate ( $\text{C}_5\text{H}_8\text{O}_2$ , 99%, MMA) and acrylic acid ( $\text{C}_3\text{H}_4\text{O}_2$ , 99%, AA), butyl acrylate ( $\text{C}_7\text{H}_{12}\text{O}_2$ , 99%, BA), allyl methacrylate ( $\text{C}_7\text{H}_{10}\text{O}_2$ , 98%, AMA), glycidyl methacrylate ( $\text{C}_7\text{H}_{10}\text{O}_3$ , 97%, GMA) were purchased from Aldrich Co. Phenolic inhibitor in all these monomers was removed by basic alumina column. No turbidity developed when a drop of monomer was added to excess hexane. Aluminum oxide ( $\text{Al}_2\text{O}_3$ , activated, basic, ~150 mesh, 58 Å), potassium persulfate ( $\text{K}_2\text{S}_2\text{O}_8$ , 99%, KPS), were purchased and used without purification. Deionized water having resistivity (18 $\Omega$ -cm) was used as a reaction medium. Nylon support was obtained from Cuno, (Meriden, Conn., Cat. No. NM827-02-020SP). This is a positively charged, an isotropic microporous nylon 66 membrane with a nominal pore size of 0.2  $\mu\text{m}$ . Cationic surfactant (Arquad 2C-75, Akzo Chemie America, McCook, IL), mixed bed ion-exchange resin ((Bio-Rad analytical grade mixed bed resin, AG501-X\* Bio-Rad Laboratories, Hercules, CA), and 2,2,4-trimethyl-1,3-pentanediol monoisobutyrate (Texanol, 99%, isomeric

mixture, Sigma-Aldrich) were used as received. Thin Mylar films with thickness in the range of 120-130  $\mu\text{m}$  were obtained from Fralock (CA).

**Particle Size Measurements.** Particle size distributions were measured by scanning electron microscopy (SEM, JSM-6360, JEOL), dynamic light scattering (DLS, Malvern HPPS 3.1 instrument equipped with a He-Ne, 3.0 mW, 633 nm laser) and by atomic force microscopy (Veeco, multimode, scanning probe microscope V (SPM), California). A copolymer dispersion of 5-6 drops was diluted to 10 mL with DI water and filtered through cotton for DLS measurements. SEM samples were prepared by placing two drops of diluted dispersion onto freshly cleaved mica sheet (1cm)<sup>2</sup> mounted on an aluminum stub, drying at room temperature and coating with 10-15 nm of gold. The SEM accelerating voltage applied was 5 kV. AFM samples were prepared by placing 2-3 drops of diluted polymer latex on to newly cleaved mica sheet (1 cm)<sup>2</sup> mounted on a steel sample puck using a small piece of adhesive tape, and dried at room temperature. Size measurements were performed with commercial silicon cantilevers (UltraSharp, MikroMasch) with a tip radius of ~10 nm. Mean diameters of 50 particles were calculated from SEM and AFM images.

**Polymerization.** The latex dispersions were prepared by emulsion polymerization at 80 °C using potassium persulfate as an initiator. All the polymerizations were carried out in a 250-mL round bottom, four-neck flask fitted with a mechanical stirrer with a Teflon blade, condenser, addition funnel, syringe pumps and thermometer. Care was taken to ensure that the stirrer was at the same distance (0.5 cm) from the bottom of the reactor for each polymerization. The stirring rate was controlled at 300 rpm. A number of

runs were made with various monomer and initiator concentrations using batch, seeded, and starved semi-continuous polymerizations.

**Batch Polymerization (1).**<sup>22</sup> Methyl methacrylate (MMA) was used to synthesize PMMA seed latex from soapless batch emulsion polymerization. The monomer (MMA, 15.4 g) and water (150.0 g) were charged to the reactor. Nitrogen was bubbled through the mixture for about 30 min at room temperature in order to displace dissolved oxygen. The mixture was heated to 80 °C over 30 min. Potassium persulfate solution (0.111 g in 2 mL DI water) was added and reaction went on for 1 h, completing the seed stage of polymerization with 10 wt% solids.

**Seeded Emulsion Polymerization (2).** Seed latex and MMA were used to synthesize submicron seed growth latex by soapless seeded emulsion polymerization. In the soapless seeded emulsion polymerization, MMA (10.0 g) was added into the seed latex dispersion of 50.0 g (1) and the seeds were swollen for 24 h at room temperature with mechanical stirring under nitrogen.<sup>22-23</sup> Then, the reaction system was heated in an oil bath at 80 °C under nitrogen with continuous mechanical stirring. Potassium persulfate (0.05 g in 2 mL DI water) solution was added into reactor and polymerization went on for 1 h, completing the seeded stage of polymerization with 4.62 wt% solids.

**Starved Semi-Continuous Polymerization (3).** Seed growth latex (2) was filtered twice through a cotton plug. Seed growth core (2) dispersion (17.2 g) and water (55.3 g) were charged to the reactor and then deoxygenated by bubbling with nitrogen for 30 min and stirred mechanically at 300 rpm in an 80 °C oil bath. Aqueous potassium persulfate solution (0.044 g in 2 mL DI water) was added and heating was continued for 5 min to begin the generation of radicals. Shell monomers were measured using

microsyringes and added into the reactor through a ¼ -in. stainless steel tube located near the shaft. The syringe pump was started and 500 mg (59 %) of methyl methacrylate, 33 mg (4.0 %) of allyl methacrylate, 32 mg (3.8 %) of acrylic acid, 130 mg (15.6 %) of glycidyl methacrylate and 148 mg (17.7 %) of butyl acrylate were fed in continuous stream for 30 min at a constant feed rate of 0.07 mL/min. The mixture was kept under nitrogen until polymerization was finished. The stable emulsion was obtained after 1 h and filtered through a cotton plug.

### **Colloidal Crystalline Filters**

**Gravitational Sedimentation and Solvent Evaporation.**<sup>9</sup> Nylon support was obtained from Cuno, (Meriden, Conn., Cat. No. NM827-02-020SP). This is a positively charged, an isotropic microporous nylon 66 membrane with a nominal pore size of 0.2 µm and with rough surface, The 0.2 µm nylon support was wetted by filtration to place the particles. For this purpose, nylon support was put in a place with Teflon O-ring in a filtration cell of 4.7 cm wide and 20 cm deep. Methanol/water (vol ratio: 1/1, 100 mL) solution was twice passed through a filter under 2 psi pressure to ensure that all the pores are wet. The wetted filter was washed with 50 mL of 0.2 wt % cationic surfactant (Arquad 2C-75) in 1:1 volume ratio of methanol/water. This prewashing of nylon substrate makes it possible to position the particles smaller than the pores of substrate on the top surface and also increases the charge interaction between the substrate surface and anionic latex particles. This preconditioned nylon substrate was put in a place with a Teflon O-ring in a Teflon well for 4.7 cm wide and 3.0 cm deep to pack LCM.

The diluted PMMA core-shell latex dispersion of 10-40 mL (0.6 wt %) was shaken with 60-240 mg of mixed bed ion-exchange resin for an hour in a mechanical shaker to remove salts and surfactants from the latex. This latex dispersion was filtered through a cotton plug. Teflon well containing preconditioned nylon substrate was placed on noise dampened table to minimize the vibrations that could hamper the particle packing. Ion-exchange treated latex dispersion of 10-20 mL was transferred to Teflon well by syringe and the solvent was allowed to evaporate for 24-48 h at room temperature. This method formed 3D colloidal crystalline membranes. Similar experiments were also performed with the dispersions containing 10 wt % Texanol relative to the weight of the particles.

**Stabilization by Thermal Annealing.**<sup>9,15-17</sup> This method is based on the interdiffusion and entanglement of the polymer chains between the particles as well as a chemical reaction at the point of contact forming a covalent linkage. Annealing the PMMA core-shell latex particles at 120 °C<sup>9</sup> for one hour causes the limited coalescence of the particles but not to flow to fill in the pores (shown in Figure 9). Residual water in the array obscures the actual temperature it reaches during the annealing. At the same time the reaction of epoxy group of GMA occurs with carboxylic group of AA to form an ester linkage<sup>15-17</sup> which will presumably interconnect the particles in the array (shown in Figure 9).

**Fluidic Cell Approach by Sonication Assisted Packing.**<sup>18-21</sup> The packing cell was a gasket-type structure shown in Figure 10 (a), constructed from two flat glass substrates (2.5 x 2.5 cm<sup>2</sup> area), a square frame (0.4 x 0.4 cm<sup>2</sup> area) of Mylar film of 130 μm thickness and tightened with binder clips. Thickness of the LCM was controlled by

thickness of the Mylar film, which can easily be changed by using different Mylar films. A small hole of 3 mm in diameter was generated on the top glass substrate by etching the glass surface using hydrofluoric acid (HF) treatment, and a glass tube 6 mm in diameter was attached to the glass substrate using an epoxy adhesive. Mylar film was rinsed with DI water and wiped with a piece of soft paper to provide channels for retaining the particles and letting the solvent flow through. The cell was placed on the edge of the sonicator.

An aqueous PMMA core-shell latex dispersion (6.0  $\mu$ L, 4.62 wt %) was diluted to 0.50 mL with DI water. This diluted dispersion (0.50 mL, 0.05 wt %) was injected into the cell, and a positive pressure was applied to the glass tube to force the solvent (water) to flow through the channels. The latex particles accumulated at the bottom of the cell under continued sonication (Figure 10 b) to pack into close-packed lattice. When the dispersion of latex particles had almost gone from the glass tube, the cell was placed in an oven at 70 °C for 2-3 h to evaporate the remaining water. After cooling to room temperature, the top substrate was removed to obtain the colloidal crystalline assembly of PMMA core-shell latex for surface characterization.

**Characterization by Microscopy.** Scanning electron micrographs of the top surfaces of the membranes were obtained from JSM-6360, JEOL instrument on samples coated with a 15-25 nm layer of gold. Cross-sections were prepared by cleaving the membrane with hands or cut with a razor blade.



## References

1. Shunchao, Gu.; Hiromitsu, A.; Daisuke, N.; Yoshio, K.; Mikio K. *Langmuir* **2004**, *20(19)*, 7548-7951.
2. Ono, H.; Jidai, E. *Colloid.Polym. Sci.* **1976**, *254(1)*, 17-24.
3. Taner, T.; Oguz, O.; Cetin, S. I. *J. Appl. Polym. Sci.* **1996**, *61(3)*, 485-493.
4. Pei, Li.; Junmin, Z.; Panya, S.; Harris, F. W. *J. Dispersion Sci. Technol.* **2003**, *24(3 & 4)*, 607-613.
5. Ono, H.; Jidai, E.; Akira, F. *J. Phys. Chem.* **1975**, *79(19)*, 2020-4.
6. Xu, Z.; Ford, W. T. *Macromolecules* **2002**, *35(20)*, 7662-7668.
7. El-Aasser, M. S.; Sudol, E. D. *Emulsion Polymerization and Emulsion Polymers*; Lovell, P. A., El-Aasser, M. S., Eds.; Wiley: Chichester, **1997**.
8. Slomkowski, S. *Prog. Polym. Sci.* **1998**, *23*, 815-874.
9. Jons, S.; Ries, P.; McDonald, C. J. *J. Membr. Sci.* **1999**, *155(1)*, 79-99.
10. Grawe, J. R.; Bufkin, G. B. *J. Coatings Technol.* **1978**, *50(641)*, 41-55.
11. Grawe, J. R.; Bufkin, G. B. *J. Coatings Technol.* **1978**, *50(643)*, 67-83.
12. Grawe, J. R.; Bufkin, G. B. *J. Coatings Technol.* **1978**, *50(644)*, 83-109.
13. Grawe, J. R.; Bufkin, G. B. *J. Coatings Technol.* **1978**, *50(645)*, 70-100.
14. Grawe, J. R.; Bufkin, G. B. *J. Coatings Technol.* **1978**, *50(647)*, 65-96.
15. Shecter, L.; Wynstra, J. *Ind. Eng. Chem.* **1956**, *48*, 86-93.
16. Madec, J. P.; Marechal, E. *Adv. Polym. Sci.* **1985**, *71*, 153-261.
17. Magnet, S.; Guillot, J.; Guyot, A.; Pichot, C. *Prog. Org. Coatings.* **1992**, *20*, 73-80.
18. Park, S. H.; Qin, D.; Xia, Y. *Adv. Mater.* **1998**, *10*, 1028-1032.

19. Park, S. H.; Xia, Y. *Langmuir*. **1999**, *15*, 266-273.
20. Gates, B.; Yin, Y.; Xia, Y. *Chem. Mater.* **1999**, *11*, 2827-2836.
21. Lu, Y.; Yin, Y.; Gates, B.; Xia, Y. *Langmuir*. **2001**, *17*, 6344-6350.
22. Lee, C. F. *Polymer* **2000**, *41*, 1337-1334.
23. Lee, C. F. *Colloid. Polym. Sci.* **2002**, *280*, 116-123.

## VITA

Rangarani Karnati

Candidate for the Degree of

Doctor of philosophy

Thesis: POLYMER COLLOIDS FOR CATALYSIS IN FLUOROUS MEDIA AND FOR COLLOIDAL CRYSTALLINE ARRAYS

Major Field: Chemistry

Biographical:

Personal Data: Born in Gannavaram, India, July 1966, daughter of Venkata Subbarao Cheethirala and Chenchulakshmi. Married to Dr. Visheweshwarrao Karnati on June 25, 1997.

Education: Received Bachelor of Science Degree in Chemistry from Nagarjuna University in May, 1986; Master of Science Degree in Synthetic Organic Chemistry from Andhra University in August, 1990; Master of Technology in Bio-technology from Jawaharlal Nehru Technological University in December, 1993; completed requirements for the Doctor of Philosophy Degree at Oklahoma State University in December, 2008.

Experience: Lecturer and Head of the Dept of Chemistry at Maitreyi Degree College for Women, Hyderabad, December, 1993 to December, 2001; Teaching Assistant, Department of Chemistry, Oklahoma State University, January, 2002 to December, 2005, Research Assistant, Department of Chemistry, Oklahoma State University, January, 2006 to August, 2008.

Professional Memberships: American Chemical Society.

Name: Rangarani Karnati

Date of Degree: May, 2009

Institution: Oklahoma State University

Location: Stillwater, Oklahoma

Title of Study: POLYMER COLLOIDS FOR CATALYSIS IN FLUOROUS MEDIA  
AND FOR COLLOIDAL CRYSTALLINE ARRAYS

Pages in Study: 85

Candidate for the Degree of Doctor of Philosophy

Major Field: Chemistry

Scope and Method of Study: Monodisperse charged polymer colloids in aqueous and non-aqueous dispersions have potential applications as membranes and catalysts. We chose poly(ethylhexyl methacrylate) particles containing quaternary ammonium ions and poly(methyl methacrylate) polymer particles for the catalytic and colloidal crystalline filter fabrication applications. Micron sized poly(ethylhexyl methacrylate) (EHMA) cross-linked copolymers in fluorinated solvents were synthesized by dispersion polymerization using microwave heating for the catalytic applications. Sub-micron sized poly(methyl methacrylate) (PMMA) core-shell latexes in aqueous media were made by emulsifier-free emulsion polymerization for colloidal crystal films (CCF) making.

Findings and Conclusions:

Cationic EHMA copolymers slightly increased the hydrolysis of *p*-nitrophenyl hexanoate in fluorous media compared to the control experiment which lacked the polymer particles. PMMA CCF's fabricated by gravitational sedimentation method contained monodisperse FCC packed domains of 5-10  $\mu\text{m}$ , point defects, and grain boundaries.

ADVISER'S APPROVAL: Warren T. Ford

---